UTILIZATION OF WASTE METARIALS FROM IRON-STEEL AND ZINC INDUSTRIES FOR SORPTION OF HYDROGEN SULFIDE AT HIGH CONCENTRATIONS

A THESIS SUBMITTED TO
THE GRADUATE SCHOOL OF NATURAL AND APPLIED SCIENCES
OF
MIDDLE EAST TECHNICAL UNIVERSITY

BY

EBRU HARMANCI

IN PARTIAL FULFILLMENT OF THE REQUIREMENTS FOR
THE DEGREE OF MASTER OF SCIENCE
IN
ENVIRONMENTAL ENGINEERING

JULY 2004

Approval of the Graduate School of Natural and Applied Sciences

Prof. Dr. Canan Özgen
Director

I certify that this thesis satisfies all the requirements as a thesis for the degree of Master of Science.

Prof. Dr. Filiz B. Dilek
Head of Department

This is to certify that we have read this thesis and that in our opinion it is fully adequate, in scope and quality, as a thesis for the degree of Master of Science.

Prof. Dr. Aysel Atımtay
Supervisor

Examining Committee Members

Assist. Prof. Dr. İpek İmamoğlu (METU, ENVE) _____

Prof. Dr. Aysel Atımtay (METU, ENVE) _____

Prof. Dr. Yavuz Topkaya (METU, METE) _____

Assoc. Prof. Dr. Mustafa Oğuz (METU, ENVE) _____

Instructor Dr. Cevdet Öztin (METU, CHE) _____

I hereby declare that all information in this document has been obtained and presented in accordance with academic rules and ethical conduct. I also declare that, as required by these rules and conduct, I have fully cited and referenced all material and results that are not original to this work.

Name, Last name : Ebru HARMANCI

Signature :

ABSTRACT

UTILIZATION OF WASTE MATERIALS FROM IRON-STEEL AND ZINC INDUSTRIES FOR SORPTION OF HYDROGEN SULFIDE AT HIGH CONCENTRATIONS

Harmancı, Ebru

M.S., Department of Environmental Engineering

Supervisor: Prof. Dr. Aysel Atımtay

July 2004, 98 pages

The slags from iron-steel and zinc industries are rich in metal oxide contents like FeO, MnO, CaO. However, these slags are not used extensively, except some usage in the cement industry. These slags can be used in removing H_2S from waste gases from different industrial sources. The purpose of this research is to study the effect of initial concentration of H_2S on the capacity and sorbent efficiency of waste materials from iron-steel and zinc industries.

Experiments were conducted in a 25 mm-quartz reactor with simulated gases containing H_2S as reactive gas. Breakthrough curves for sulfidation reactions were obtained for 3000 ppmv, 4000 ppmv and 5000 ppmv initial H_2S concentrations at the reaction temperature range of 500°C–700°C.

According to the results obtained from the experiments, the H_2S removal capacity of both slags increased with increasing reaction temperature, however, the H_2S removal capacity of the slags decreases as the initial H_2S concentration increases.

Cyclic sulfidation and regeneration tests were applied to both steel and zinc slags in order to determine the regenerability of the slags. In cyclic tests, zinc slag gave better results than steel slag.

A "Deactivation Model" was used in order to fit the breakthrough curves obtained experimentally to the breakthrough curves predicted from the deactivation model. A very good fit was obtained for both steel and zinc slags.

Zinc slag was shown to be more suitable for gas cleanup than steel slag taking into account its high H_2S removal efficiency, regenerability and low cost (almost free of charge).

Keywords: H_2S removal, Slag , Deactivation model

ÖZ

DEMİR-ÇELİK VE ÇİNKO ENDÜSTRİLERİNDEN ÇIKAN ATIK MADDELERİN YÜKSEK KONSANTRASYONLU KÜKÜRTLÜ HİDROJEN GAZI GİDERİLMESİNDE KULLANILMASI

Harmancı, Ebru
Yüksek Lisans, Çevre Mühendisliği Bölümü
Tez Yöneticisi: Prof. Dr. Aysel Atımtay

Temmuz 2004, 98 sayfa

Demir-çelik ve çinko endüstrilerinden çıkan cüruflar FeO, MnO, CaO gibi metal oksitleri açısından zengindir. Buna rağmen, bu cüruflar çimento endüstrisi haricinde yaygın olarak kullanılmamaktadır. Bu atıklardan çeşitli endüstrilerden çıkan ve H_2S içeren atık gazların temizlenmesinde yararlanılabilir. Bu araştırmanın amacı, demir-çelik ve çinko endüstrilerinden çıkan cüruf sorbent olarak kullanıldığında, H_2S gazı başlangıç konsantrasyonunun sorbent kapasitesi ve verimi üzerindeki etkisini incelemektir.

Deneyler, iç çapı 25 mm olan kuartz bir reaktörde reaktif gaz olarak H_2S içeren simüle edilmiş gaz karışımları ile yapılmıştır. 500°C-700°C reaksiyon sıcaklıklarında, 3000 ppmv, 4000 ppmv ve 5000 ppmv başlangıç H_2S konsantrasyonları için sülfidasyon kırılma eğrileri elde edilmiştir.

Deneylerden elde edilen sonuçlara göre, reaksiyon sıcaklığının artmasıyla her iki cürufun da H_2S giderim kapasiteleri artmaktadır. Ancak, başlangıç H_2S konsantrasyonu arttıkça cürufların H_2S giderim kapasiteleri azalmaktadır.

Hem çelikhane, hem de çinko cürufunun rejenerasyona uygun olup olmadığını tespit etmek amacıyla ardışık sülfidasyon ve rejenerasyon deneyleri yapılmıştır. Ardışık testlerde çinko cürufu çelikhane cürufundan daha iyi sonuçlar vermiştir.

Deneysel olarak elde edilen kırılma eğrileri, "deaktivasyon model"ine göre hesaplanan kırılma eğrileri ile karşılaştırılmıştır. Hem çelikhane, hem de çinko cürufu için çok iyi bir uyum elde edilmiştir.

Yüksek H_2S giderim verimliliği, rejenerasyona uygun olması ve düşük maliyetli (hatta ücretsiz) olması nedeniyle, gaz temizlenmesinde çinko cürufunun çelikhane cürufundan daha uygun olduğu saptanmıştır.

Anahtar Kelimeler: H_2S giderimi, Cüruf, Deaktivasyon modeli

To My Family

ACKNOWLEDGEMENTS

I wish to express my deepest gratitude to my supervisor Prof. Dr. Aysel Atımtay for her guidance, advices, criticisms and encouragement and insight throughout this thesis.

I would like to thank Mr. Cengiz Tan for helping me in the analysis with the Scanning Electron Microscope. Mr. Necmi Avcı is gratefully acknowledged for his assistance during the XRD analyses. I would also like to extend my thanks to the technicians in our Department, Mr. Sami Beştepe, Mr. Kemal Demirtaş, Mr. Murat Dündar and Mr. Ramazan Demir for their support during this thesis work. I would like to thank my friends Y.Bahadır Duygulu, Baran Görmez, İrem Önoğlu, R.Kaya Göktaş and Ahmet Türküm for their friendship and support throughout this thesis.

I would like to express my deepest gratitude to my family for their endless support and encouragement. I would also like to express my special thanks to my husband İbrahim for bearing up with me throughout this study and giving me his endless support.

TABLE OF CONTENTS

PLAGIARISM iii
ABSTRACT iv
ÖZ vi
ACKNOWLEDGEMENTS ix
TABLE OF CONTENTS x
LIST OF TABLES xiii
LIST OF FIGURES xiv
LIST OF ABBREVIATIONS xvii
CHAPTER
1. INTRODUCTION 1
1.1 General 1
1.2 Objectives of the Study 4
2. LITERATURE SURVEY 5
2.1 Coal Gasification 5
2.1.1 Types of Gasifiers 6
2.2 Integrated Gasification Combined Cycle (IGCC) 8
2.3 Hot Coal Gas Cleanup 12
2.3.1 High Temperature Desulfurization Sorbents 14
2.3.1.1 Metal Oxides 15
2.3.1.1.1 Iron Oxide 19
2.3.1.1.2 Zinc Oxide 21

2.4 Industrial Wastes as Desulfurization Sorbent 23
2.4.1 Steel Slag 24
2.4.2 Zinc Slag 25
2.5 Deactivation Model 26
3. EXPERIMENTAL SECTION 30
3.1 Sorbent Properties 30
3.1.1 Physical Characterization of the Sorbent 30
3.1.1.1 Steel Slag 31
3.1.1.2 Zinc Slag 35
3.1.2 Chemical Characterization of the Sorbent 36
3.1.2.1 Steel Slag 39
3.1.2.2 Zinc Slag 40
3.2 Experimental Setup 42
3.3 Experimental Procedure 44
3.3.1 Sulfidation Experiments 46
3.3.2 Regeneration Experiments and Cyclic Tests 47
4. RESULTS AND DISCUSSION 48
4.1 Sulfidation Experiments 48
4.1.1 Sulfidation Experiments with Steel Slag 49
4.1.2 Sulfidation Experiments with Zinc Slag 56
4.2 Cyclic Tests 63
4.2.1 Cyclic Tests of Steel Slag 63
4.2.2 Cyclic Tests of Zinc Slag 65
4.3 Physical Characterization After Sulfidation 68
4.3.1 Steel Slag 68
4.3.2 Zinc Slag 71
4.4 Chemical Characterization After Sulfidation 72
4.5 Deactivation Model Predictions 73
4.5.1 Regression Analysis for Steel Slag 75

4.5.2 Regression Analysis for Zinc Slag 77
4.6 Comparison of Results with the Data from Literature 80
5. CONCLUSIONS 83
REFERENCES 85
APPENDICES
A. CALIBRATION CURVES AND METHOD USED IN GC 92
B. CALCULATION OF SORPTION CAPACITY 96

LIST OF TABLES

Table 2.1 Emissions from Different Systems [18] 12
Table 2.2 Chemical Composition of Steel Slag at KARDEMİR [3] 25
Table 2.3 The Typical Analysis of Waelz Furnace Slag [37] 26
Table 3.1 BET Surface Areas of Fresh Steel Slag [3] 31
Table 3.2 Mercury Porosimetry Analysis of Steel Slag [3] 32
Table 3.3 Mercury Porosimetry Analysis of Fresh Zinc Slag [3] 36
Table 3.4 Chemical Analysis of Steel Slag (% by wt.) [3] 39
Table 3.5 Chemical Analysis of Zinc Slag [3] 41
Table 3.6 Inlet Gas Compositions for Sulfidation Experiments 46
Table 4.1 Sorption Capacities of Steel Slag 56
Table 4.2 Sorption Capacities of Zinc Slag 62
Table 4.3 Sorbent Capacities of Steel Slag During Cyclic Test 66
Table 4.4 Sorbent Capacities of Zinc Slag During Cyclic Test 68
Table 4.5 Rate Parameters for Steel Slag 75
Table 4.6 Activation Energies of Steel Slag 77
Table 4.7 Rate Parameters for Zinc Slag 78
Table 4.8 Activation Energies of Zinc Slag 78
Table 4.9 Comparison of Sorption Capacities of Different Sorbents 81

LIST OF FIGURES

Figure 2.1 Types and Temperature Profiles of Coal Gasifiers [5].....7
Figure 2.2 Schematic Diagram of IGCC System [3].....9
Figure 2.3 Stable Solid Phases of the Eleven Elements [25].....16
Figure 2.4 Desulfurization Potentials of Eleven Metals [25] 17
Figure 2.5 Sulfur Removal Efficiencies of Several Metal Oxides [19].....18
Figure 3.1 Cumulative Pore Distributions of 2-3 mm Steel Slag [3].....33
Figure 3.2 Incremental Intrusion Volumes of 2-3 mm Steel Slag [3].....33
Figure 3.3a SEM Photographs of 2-3 mm Fresh Steel Slag (x2000) [3].....34
Figure 3.3b SEM Photographs of 2-3 mm Fresh Steel Slag (x4500) [3].....35
Figure 3.4 Cumulative Pore Distributions of 2-3 mm Zinc Slag [3].....37
Figure 3.5 Differential Intrusion Volumes of 2-3 mm Zinc Slag [3].....37
Figure 3.6a SEM Photographs of 2-3 mm Zinc Slag [3] 38
Figure 3.6b SEM Photographs of 2-3 mm Zinc Slag [3] 38
Figure 3.7 XRD Analyses of 2-3 mm Fresh Steel Slag [3].....40
Figure 3.8 XRD Analyses of 2-3 mm Zinc Slag [3] 41
Figure 3.9 Schematic Diagram of Experimental Setup [3] 42
Figure 4.1 Breakthrough Curves for H_2S at Different Temperatures with 3000 ppmv Inlet Concentration (steel slag as sorbent) 50
Figure 4.2 Breakthrough Curves for H_2S at Different Temperatures with 4000 ppmv Inlet Concentration (steel slag as sorbent) 51
Figure 4.3 Breakthrough Curves for H_2S at Different Temperatures with 5000 ppmv Inlet Concentration (steel slag as sorbent) 52

Figure 4.4 Breakthrough Curves for H_2S at 700°C Showing the Effect of Inlet Concentration (steel slag as sorbent).....53
Figure 4.5 Breakthrough Curves for H_2S at 500°C (steel slag as sorbent) 54
Figure 4.6 Breakthrough Curves for H_2S at 600°C (steel slag as sorbent) 55
Figure 4.7 Breakthrough Curves for H_2S at Different Temperatures with 3000 ppmv Inlet Concentration (zinc slag as sorbent).....58
Figure 4.8 Breakthrough Curves for H_2S at Different Temperatures with 4000 ppmv Inlet Concentration (zinc slag as sorbent).....58
Figure 4.9 Breakthrough Curves for H_2S at Different Temperatures with 5000 ppmv Inlet Concentration (zinc slag as sorbent).....59
Figure 4.10 Breakthrough Curves for H_2S at 600°C Showing the Effect of Inlet Concentration (zinc slag as sorbent) 60
Figure 4.11 Breakthrough Curves for H_2S at 600°C (zinc slag as sorbent).....61
Figure 4.12 Breakthrough Curves for H_2S for Four Successive Sulfidation at 500°C with 4000 ppmv Inlet Concentration 64
Figure 4.13 Breakthrough Curves for SO_2 During Regeneration at 500°C 65
Figure 4.14 Breakthrough Curves for H_2S for Four Successive Sulfidation at 500°C with 5000 ppmv Inlet Concentration 66
Figure 4.15 Breakthrough Curves for SO_2 During Regeneration at 500°C 67
Figure 4.16a SEM Photographs of Steel Slag After Sulfidation with Inlet Concentration of 4000 ppmv H_2S 69
Figure 4.16b SEM Photographs of Steel Slag After Sulfidation with Inlet Concentration of 4000 ppmv H_2S 70
Figure 4.16c SEM Photographs of Steel Slag After Sulfidation with Inlet Concentration of 4000 ppmv H_2S 70
Figure 4.17a SEM Photographs of Zinc Slag After Sulfidation with Inlet Concentration of 5000 ppmv H_2S 71
Figure 4.17b SEM Photographs of Zinc Slag After Sulfidation with Inlet Concentration of 5000 ppmv H_2S 72

Figure 4.18 XRD Graph of Steel Slag After Sulfidation at 700°C with 4000 ppmv H_2S 73
Figure 4.19 Comparison of Breakthrough Curves for 4000 ppmv H_2S at 500°C Obtained by Deactivation Model Prediction and Experimental Data 76
Figure 4.20 Comparison of Breakthrough Curves for 3000 ppmv H_2S at 700°C Obtained by Deactivation Model Prediction and Experimental Data 76
Figure 4.21 Comparison of Breakthrough Curves for 5000 ppmv H_2S at 500°C Obtained by Deactivation Model Prediction and Experimental Data 79
Figure 4.22 Comparison of Breakthrough Curves for 3000 ppmv H_2S at 600°C Obtained by Deactivation Model Prediction and Experimental Data 79
Figure A.1 Calibration Curve for H_2S.....94
Figure A.2 Calibration Curve for SO_2.....95
Figure B.1 Typical Breakthrough Curve.....96
Figure B.2 Breakthrough Curve at 500°C with 3000 ppmv H_2S (Steel Slag)..97

LIST OF ABBREVIATIONS

a	Activity of the Solid Sorbent
AAS	Atomic Absorption Spectrophotometer
C	Exit Concentration of H_2S
C_o	Inlet Concentration of H_2S
C_A	Concentration of Reactant Gas
C_{A0}	Initial Concentration of Reactant Gas
^oC	Degrees Celcius
cm	Centimeter
DOE	Department of Energy, United States
E_a	Activation Energy
g	Gram
GC	Gas Chromatograph
IGCC	Integrated Gasification Combined Cycle
kg	Kilogram
k_0	Initial Sorption Rate Constant
k_d	Deactivation Rate Constant
m	Meter
METC	Morgantown Energy Technology Center
METU	Middle East Technical University
Min	Minutes
MJ	Million Joule

ml	Milliliter
mm	millimeter
MPa	MegaPascal
PFPD	Pulsed Flame Photometric Detector
ppmv	Parts per million by volume
Q	Volumetric flowrate of gas
R	Gas Constant
SEM	Scanning Electron Microscope
TGA	Thermogravimetric Analyzer
μm	Micrometer
wt	Weight
W	Sorbent mass
XRD	X-Ray Diffraction

CHAPTER 1

INTRODUCTION

1.1 General

The Integrated Gasification Combined Cycle (IGCC) is an advanced process for power generation that is based on conversion of solid coal into a synthetic gas in a gasifier. Power generation efficiency of IGCC systems is fairly higher than that of conventional systems (55% as opposed to 30-35% in conventional systems). During gasification process, sulfur in the coal converts to mainly hydrogen sulfide and other sulfurous compounds because of the reducing condition in the gasifier. It is estimated that H_2S concentration in coal gas from a typical gasifier is about 5000 ppmv. Hydrogen sulfide can be oxidized to SO_2 and/or SO_3 in the atmosphere and these gases cause acid rain formation. Therefore, hydrogen sulfide should be removed from coal gas. In addition to that, it is known that hydrogen sulfide causes corrosion on turbine blades and other mechanical parts in the IGCC system. The allowable hydrogen sulfide concentration to be used in IGCC system shall be around 150-200 ppmv at

most [1]. Thus, it is necessary to reduce H_2S concentration in coal gas from 5000 ppmv to 150-200 ppmv.

The temperature of the coal gas at the exit of gasifier is quite high (about 500-600°C). The coal gas from the gasifier used to be cooled down before desulfurization. This is a significant energy loss considering whole IGCC system. If the coal gas can be desulfurizated at elevated temperatures, the heat efficiency of the whole IGCC system will be greatly improved. Thus, a hot gas cleanup system is necessarily required from the heat efficiency point of view whether the sulfur content of the coal is high or low.

Hot gas desulfurization mainly depends on the improvement of regenerable sorbents. Various sorbents have been developed for desulfurization of coal gas. There are some requirements for the sorbent to be used for this purpose including resistance to high reducing gas atmosphere and high temperatures, favorable thermodynamic equilibria, high reactivity with H_2S gas, structural stability and a reasonable cost. Also, the number of sulfidation/regeneration cycle should be high because once-through sorbents increase the cost of the hot gas desulfurization process.

In the literature, there are many studies related with the improvement of hot gas desulfurization sorbent. These studies show that metal oxide mixtures remove H_2S efficiently at elevated temperatures. Coal gasification process occurs at about 500-600^{o}C and most of the metal oxide sorbents can be successfully used for desulfurization at this temperature range.

The waste slag from iron and steel industry is composed mainly of metal oxide, which can be used as desulfurization sorbent at elevated temperatures. This waste slag is deposited on the area around the plant and causes environmental

pollution. So, reusing of this waste slag in desulfurization process shall prevent environmental pollution while supplying a desulfurization sorbent almost free of charge. In Turkey, there are a few integrated iron and steel plants, which produce about 1.5-2 million tons of steel slag per year. KARDEMİR, one of the integrated iron and steel, has generated about 5 million tons of steel slag over the years. This slag contains appreciable amounts of metal oxides like FeO, MnO, CaO, etc. Also, metal oxides like ZnO and FeO are present in the waste slag from zinc industry and it may be utilized as desulfurization sorbent as steel slag.

In all sorbent development studies, the purpose is to develop an economical and effective sorbent for hot gas desulfurization. Slags from iron and steel plants as well as zinc plants are economical because they are wastes of the main processes. Thus, their procurement costs are very low. Metal oxides like FeO and ZnO are proven to reduce the hydrogen sulfide concentration in the coal gas to the desired degree [2]. Steel slag and zinc slag contains large amounts of these metal oxides. These metal oxides have removed hydrogen sulfide efficiently in the previous studies [3, 4]. Therefore, steel and zinc slags are strong candidates to be used as desulfurization sorbent.

As a result, it is decided to use steel slag and zinc slag as desulfurization sorbent in our studies considering their economical viability and availability (present in high amounts) for hot gas desulfurization systems.

1.2 Objectives of the Study

This work is a continuation of the study done by Sarıçiçek [3] in 2002 in the Environmental Engineering Department of METU. The objectives of this study are:

- to investigate whether steel slag and zinc slag show good performance with high hyrogen sulfide concentrations for removing hydrogen sulfide at elevated temperature,

- to do the sulfidation and regeneration experiments with higher concentrations of hydrogen sulfide than Sarıçiçek [3] has used and to compare the behaviour of sorbents in this study with that in the previous study,

- to find out the optimum conditions (that is, concentration and temperature) for steel and zinc slags in removing hydrogen sulfide,

- to apply the "deactivation model" to the data obtained by experiments.

Waste steel slag was obtained from KARDEMİR, one of the integrated iron and steel plants in Turkey, and zinc slag was obtained from ÇİNKUR, the only primary zinc processing plants in Turkey, for this study.

CHAPTER 2

LITERATURE SURVEY

2.1 Coal Gasification

In conventional generation of power from coal, coal is reacted with steam and an oxidant, which is mainly oxygen or air. Carbon monoxide and hydrogen, which are combustible gases, are among the most prominent products of gasification [5].

The fate of trace elements such as sulfur and nitrogen is also important. Sulfur in coal is converted primarily to H_2S under reducing conditions of gasification. High temperatures and low pressures favor conversion of coal nitrogen to N_2 while the opposite conditions favor conversion of some of the nitrogen to NH_3. Small amounts of HCN are also formed [5].

There are some other usage areas of the coal gas rather than electricity generation. Alpert and Gluckman [6] stated that coal gas can be used as a

substitute for natural gas if subsequent downstream processes are applied to convert the CO and H_2 to methane. Also, coal gas can be a reducing gas for ore reduction or the hydrogen produced can be used in oil refineries as well (hydro treated oil fractions). Another possibility is that it can be a synthesis gas in chemical industry to produce ammonia, methanol diesel and other hydrocarbon products [7].

2.1.1 Types of Gasifiers

There is a large number of coal gasification processes, each having its own distinctive characteristics. However, essentially all gasification processes can be separated into the three classic types of reactors:

- Moving-bed reactors
- Fluidized-bed reactors
- Entrained-flow reactors

Figure 2.1 shows the three types of coal gasification reactors together with temperature profiles and location of the coal, steam and oxidant (air or oxygen) inputs and the coal gas and ash outputs [5].

Moving-bed gasifiers involve a counter-current flow of the coal and the gaseous reactants (e.g., air or steam). The coal is fed in 3-30 mm particle size. The coal with large particles moves slowly down through the bed while reacting with the gases moving up through the bed. The highest temperature in the bed is achieved near the bottom of the gasifier. The outlet gas temperatures are in the 400°C-800°C range and because of the relatively lower temperatures of the outlet gas, however, condensable tars or oils are produced [8].

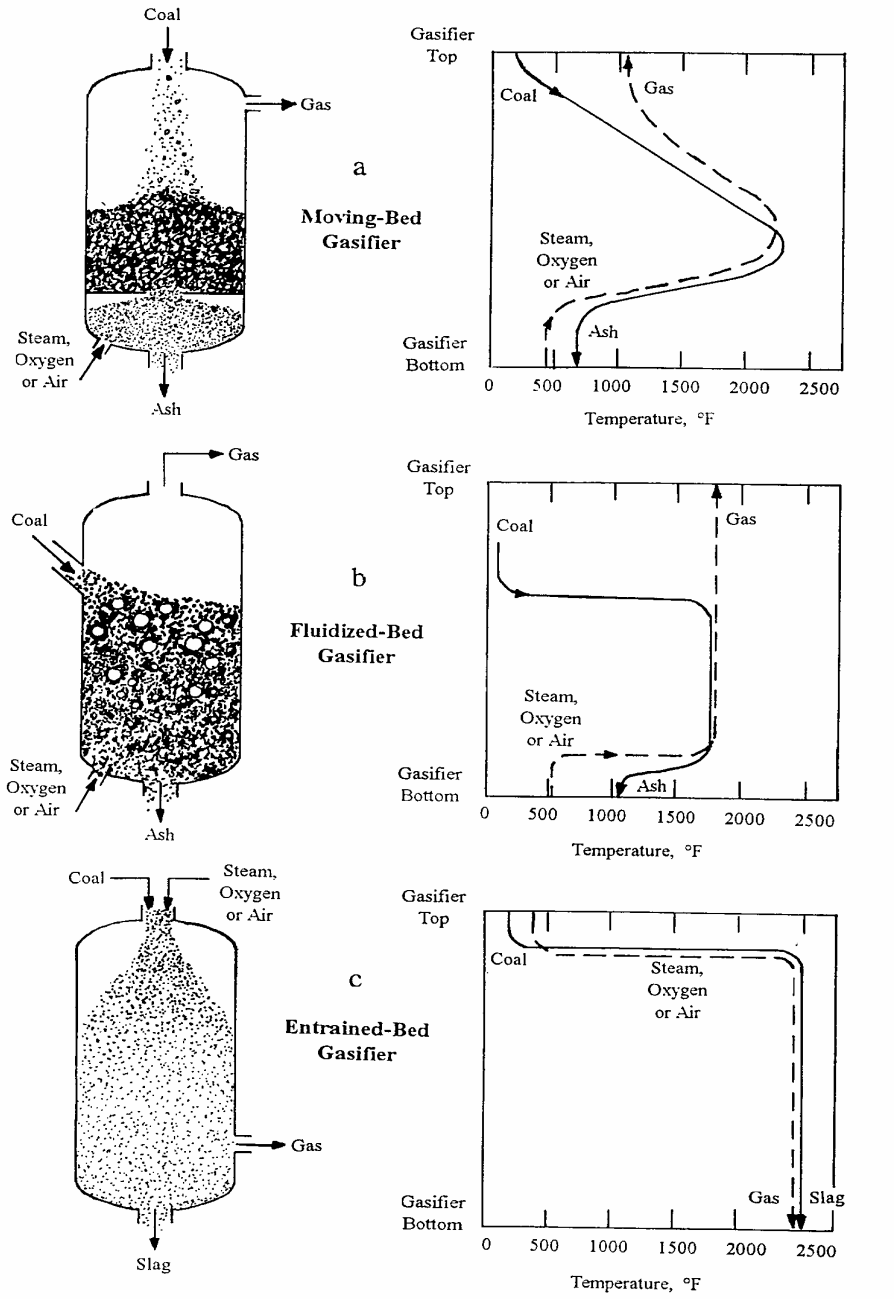

Figure 2.1 Types and Temperature Profiles of Coal Gasifiers [5]

a) Moving-Bed b) Fluidized-Bed c) Entrained-Bed

In fluidized-bed gasifiers, the reacting solids are kept in turbulent motion by a rapid updraught of air or oxygen and steam. This type of gasifiers operate within a relatively narrow temperature range, usually just below the ash fusion point to avoid bed defluidisation and the formation of tars [9]. The coal is fed in the 1-5 mm particle size. The gas temperatures are in the range 800 – 1100ºC and operate in the range of 1 to 25 bar [8].

In entrained-bed gasifiers, coal passes rapidly through the reaction zone while entrained in oxygen, steam and product gases. These gasifiers operate at higher temperatures, consequently, generate high alkali salt levels in the fuel gas as well as a sticky ash [9]. The product gas does not contain any tars and oils [6].

2.2 Integrated Gasification Combined Cycle (IGCC)

The world relies increasingly on coal as a primary energy source. All over the world most power plants burn coal to run turbines. The sulfur in coal is gasified, and every year tens of thousands of tons of sulfur are emitted into the atmosphere from chimneys of power plants. With increasing attention being paid to environmental protection, it has become clear that sulfur emission sources must be reduced [10].

Integrated Gasification Combined Cycle (IGCC) power plants are among the leading contenders for coal conversion. IGCC offers the potential of both lower cost power and lower emissions than conventional power plants with flue gas desulfurization [4]. The schematic diagram of a typical IGCC system is shown in Figure 2.2 [3].

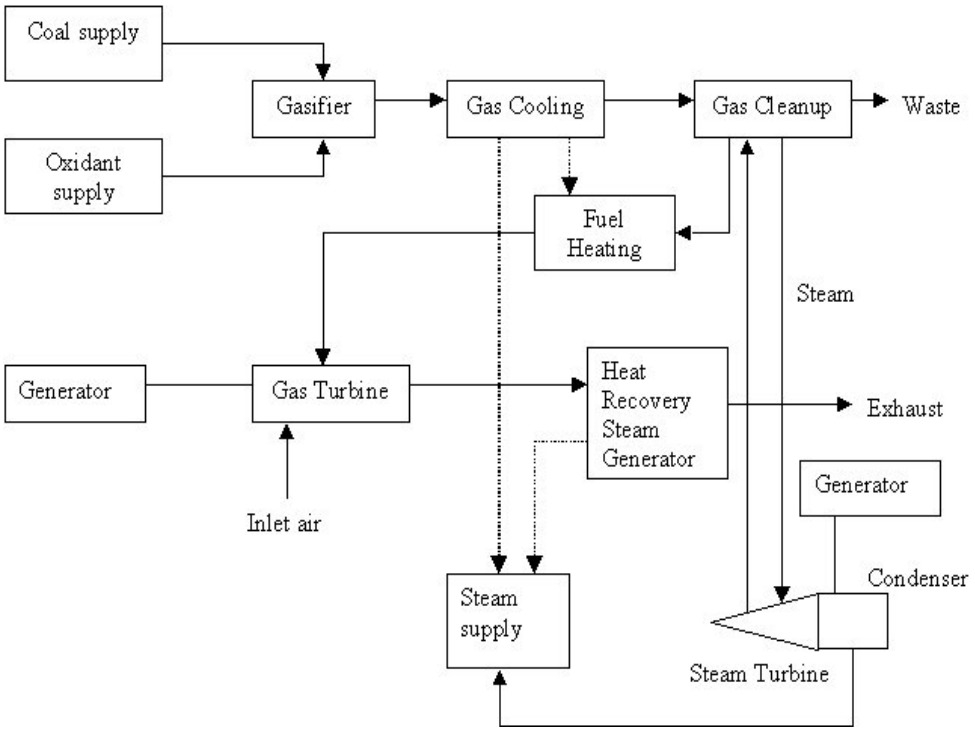

Figure 2.2 Schematic Diagram of IGCC System [3]

Coal is supplied to the gasifier with the oxidant, air or oxygen, in addition to steam or other medium for temperature control, to produce a gaseous fuel composed primarily of hydrogen, carbon monoxide, carbon dioxide, and steam. If air has been used for gasification, the product coal gas will also contain nitrogen as a diluent.

Other components present in coal in minor concentrations – such as sulfur, chlorine, organic nitrogen, and heavy metals – will end up in the coal gas as contaminants in the form of hydrogen sulfide (H_2S), hydrogen chloride (HCl), ammonia (NH_3) and trace element contaminants. Most of these contaminants will have to be removed prior to combustion in the gas turbine or prior to venting of the flue gases to the atmosphere. Cleaning of the coal gas can be

accomplished either by existing commercial low temperature cleanup technologies or at high temperature via hot gas cleanup systems.

The clean coal gases are then fully combusted to carbon dioxide and water in a gas turbine, producing electricity in the process. Some of the thermal energy of the exiting flue gas from the turbine can be recovered by heat exchange in a heat recovery steam generator, thus producing steam, which finally goes through a steam turbine for further electricity production. The combination of a gas turbine, heat recovery steam generator and steam turbine, is commonly called the combined cycle, because it combines Brayton cycle of the gas turbine with Rankine cycle of the steam turbine, with the heat recovery steam generator acting as a link between the two cycles [11]. The IGCC takes advantage of thermodynamic efficiencies by integrating the gasification cycle with the combined cycle for power generation. The result is a more efficient system [12].

IGCC system has various advantages over the other conventional systems. IGCC systems meet all projected environmental regulations, solving the compliance problems of both electric power generators and liquid fuel producers. Because they operate at higher efficiency levels than conventional fossil-fueled power plants, IGCC systems emit less CO_2 per unit of energy produced. IGCC emissions of sulfur dioxide and nitrogen oxides, gases linked to the acid rain, are a small fraction of allowable limits. While the treatment efficiency of SO_x emission in conventional systems with “scrubber” is 90 %, this efficiency can reach up to 99 % in IGCC systems. Same treatment efficiency is also valid for NO_x and particulates [13]. The economic advantages of IGCC system are its use of low-cost feedstocks, its high efficiency in resource use, its economically efficient reduction of environmental pollutants, and its integration of processes within the plant complex. Also, it delivers high-

value products. Modularity and phased construction distribute capital expenditures to meet financing requirements [6]. Modular construction also makes the plant possible for future expansions according to the increasing demands.

Other advantages of IGCC system include the absence of liquid waste problem that requires wastewater treatment. The solid waste problem in this system is also minimized because the sorbent can be regenerated and the adsorbed H_2S can be converted into commercial products like sulfuric acid or elemental sulfur [14].

Current IGCC plants operate with an efficiency of about 43%, compared to 35% for a conventional coal plant [13]. The energy conversion efficiency of IGCC systems is comparable to the conversion efficiency of natural gas combined cycle systems, which is around 52 – 54 % [15, 16]. It has been projected that a power plant based on IGCC technology will exceed 50 % energy efficiency within a decade, reducing the emissions of CO_2 greenhouse gases into the atmosphere by about 35% through this improved efficiency alone [17].

Table 2.1 [18] shows the comparison of IGCC with natural gas systems and conventional coal firing systems with respect to emissions. Although SO_2 emission of IGCC is a little higher than that of natural gas systems, IGCC has the least NO_x emission among the others. There is no mercury and particulate emission to the atmosphere.

At the exit of a typical gasifier, the temperature is about 600–800ºK. If the fuel gas can be purified at such a high temperature, the heat efficiency of the whole IGCC system will be greatly improved [10].

Table 2.1 Emissions from Different Systems [18]

Emissions	IGCC with Gas Clean-up	Natural Gas Systems	Conventional Coal Firing [a]
SO_2 (mg S/MJ)	<5 [b]	<3	50
NO_x (mg NO_2/MJ)	<50	50 – 150	100
Mercury to atmosphere (μg/MJ)	-	-	0.3
Particulates (mg/MJ)	-	-	30
Ash (% of coal feed)	12 Vitreous slag [c]	-	20 – 30 ash + gypsum [d]

[a] fluidized-bed combustion with flue-gas desulfurization

[b] more than 99% S removal

[c] non-hazardous road-filling material

[d] hazardous waste

MJ : Million Joule

2.3 Hot Coal Gas Cleanup

When coal is gasified, the sulfur in the coal reacts with steam to form hydrogen sulfide and small amounts of other sulfur-containing compounds. The typical concentration of H_2S exiting the gasifier is around 5000 ppmv [19]. Hydrogen sulfide is a toxic gas which contributes to the formation of acid rain when it is oxidized to SO_2 and/or SO_3. It is, therefore, necessary to remove as much of the hydrogen sulfide as possible from the coal gasification stream prior to

release to the atmosphere. Additionally, turbines and related equipment need to be protected from the corrosive action of sulfurous compounds in the coal gas [20]. The typical H_2S concentration that gas turbines can tolerate is about 150-200 ppmv [1].

Existing technologies to remove the coal gas contaminants are based on wet cleaning systems, which have an adverse effect on cycle efficiency, can have high capital cost and can produce an aqueous effluent requiring expensive treatment before disposal. The low operation temperature of these processes results in penalties in terms of plant efficiency and the need for treatments of water effluents [21]. The development and introduction of hot gas cleaning systems offers the potential of a lower cost approach to pollutant control with associated cycle efficiency advantages. The hot gas systems, which will replace the conventional wet gas technologies, will need to operate at 300-600°C and at pressures of 10-25 bar. In order to realize fully the cost and environmental advantages, it is essential that the systems developed give not only efficient removal of the respective pollutant but also have the reliability and availability to match the respective wet gas system [22].

Hot gas cleanup systems reduce or eliminate the need for syngas cooling prior to particulate removal and desulfurization. This improves the plant thermal efficiency and reduces or eliminates the need for heat exchangers and process condensate treatment. Thus, hot gas cleanup offers a more highly integrated system in which a major wastewater stream is eliminated [23].

Hot gas desulfurization offers energy efficiency gains over low-temperature liquid scrubbers of H_2S and avoids costly wastewater treatment. The projected cost of hot gas cleanup is approximately half that of commercially-available

cold gas desulfurization; hence, there exists high interest in developing the new process [24].

Improvement of hot gas cleanup systems (high-temperature desulfurization processes) is based on the noncatalytic gas-solid reaction between H_2S and appropriate metal oxide sorbent [25].

2.3.1 High Temperature Desulfurization Sorbents

Coal gas desulfurization to sufficiently low levels at elevated temperatures and pressures continues to be recognized as crucial to the commercialization of advanced systems such as IGCC. The implementation of hot coal gas desulfurization heavily relies on the development of regenerable sorbents, which can efficiently remove H_2S (from several thousands ppmv levels down to a few ppmv) over many cycles of sulfidation/regeneration. These sorbents must satisfy a number of requirements imposed by the IGCC process, including favorable thermodynamic equilibria during sulfidation and regeneration, relatively high sulfidation and regeneration reactivities, good mechanical strength and structural stability, environmental acceptability, and a reasonable manufacturing cost [4].

For economic viability of the process, the sorbents must retain their activity as they pass round and round the system from sulfider to regenerator. The sorbents must also retain mechanical stability with minimal attrition losses [22].

Among the sorbents investigated for high-temperature desulfurization of H_2S in a dry system, some metal oxides were found to show good potential [26].

2.3.1.1 Metal Oxides

In 1976, Westmoreland and Harrison [25] published the results obtained from a study concerned with thermodynamic screening of the high temperature desulfurization potential of 28 elements, primarily present as metal oxides. 11 out of 28 elements, namely Ba, Ca, Co, Cu, Fe, Mn, Mo, Sr, V, W, and Zn, showed thermodynamic feasibility for high temperature desulfurization. The stable solid phases of those metals are given in Figure 2.3 [25]. According to that figure, Co, Cu, Fe, Mn, Mo, V, W, and Zn can be used in the temperature up to 650°C.

Desulfurization potentials of mostly tried elements for H_2S desulfurization sorbent is given in the Figure 2.4 [25]. It is shown that Zn has the highest desulfurization potential among the other elements however it decreases sharply after 850°C.

From these group of sorbents, most attention has been paid to the materials containing Fe, Mn, Ca, and Zn. Their sulfur removal efficiencies in the temperature range of 400 – 1000ºC are given in Figure 2.5 [19]. It is seen that zinc ferrite and zinc oxide have about 98% sulfur removal efficiency in the temperature range of about 400 – 600ºC. The sulfur removal efficiency of iron oxide is about 90 % in the temperature range of 350 – 700ºC, which is quite larger range compared to the zinc oxide although the sulfur removal efficiency of iron oxide is a little lower than that of zinc oxide. Ca-based sorbents have about 95 % sulfur removal efficiency at temperatures between 750 – 900°C.

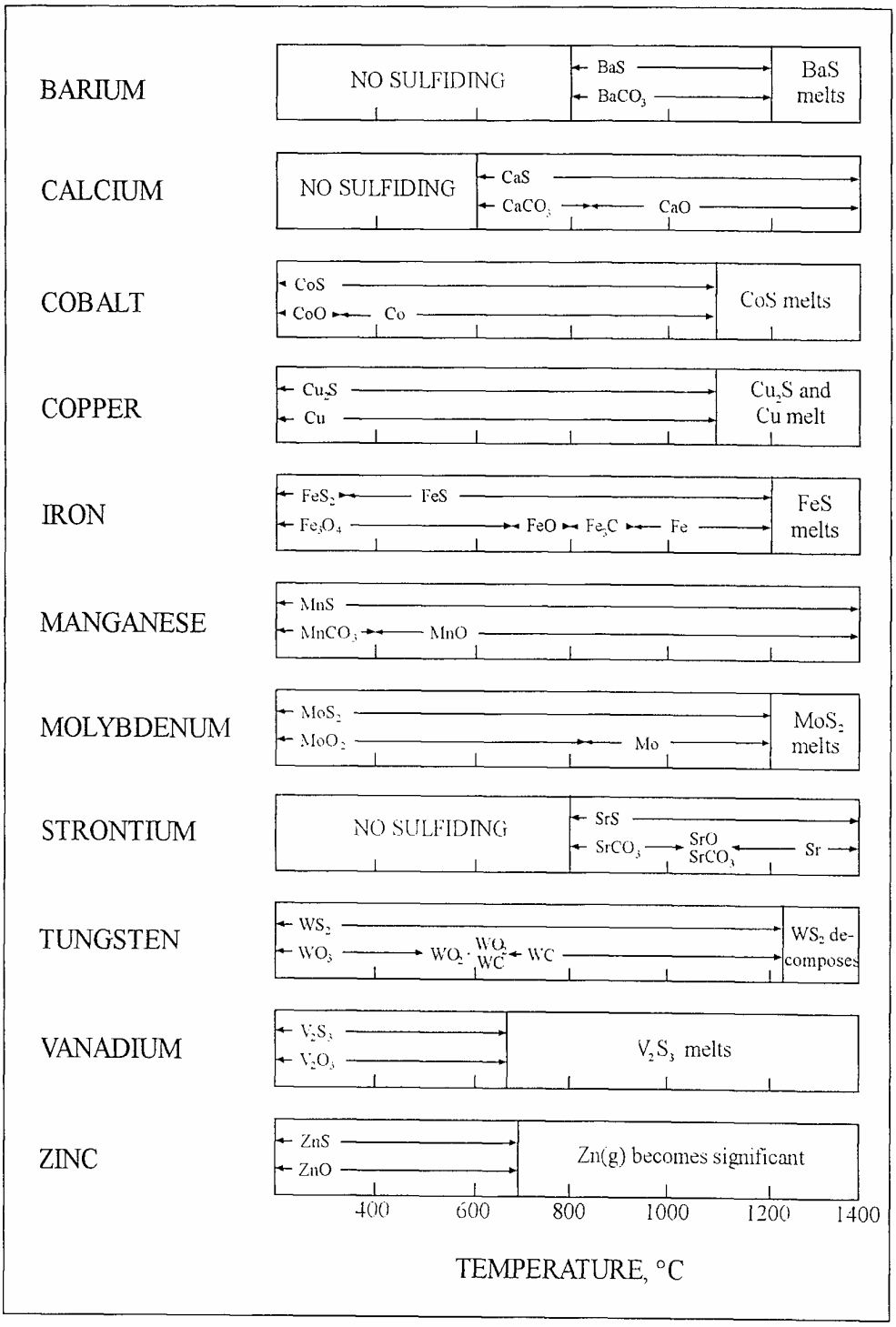

Figure 2.3 Stable Solid Phases of the Eleven Elements [25]

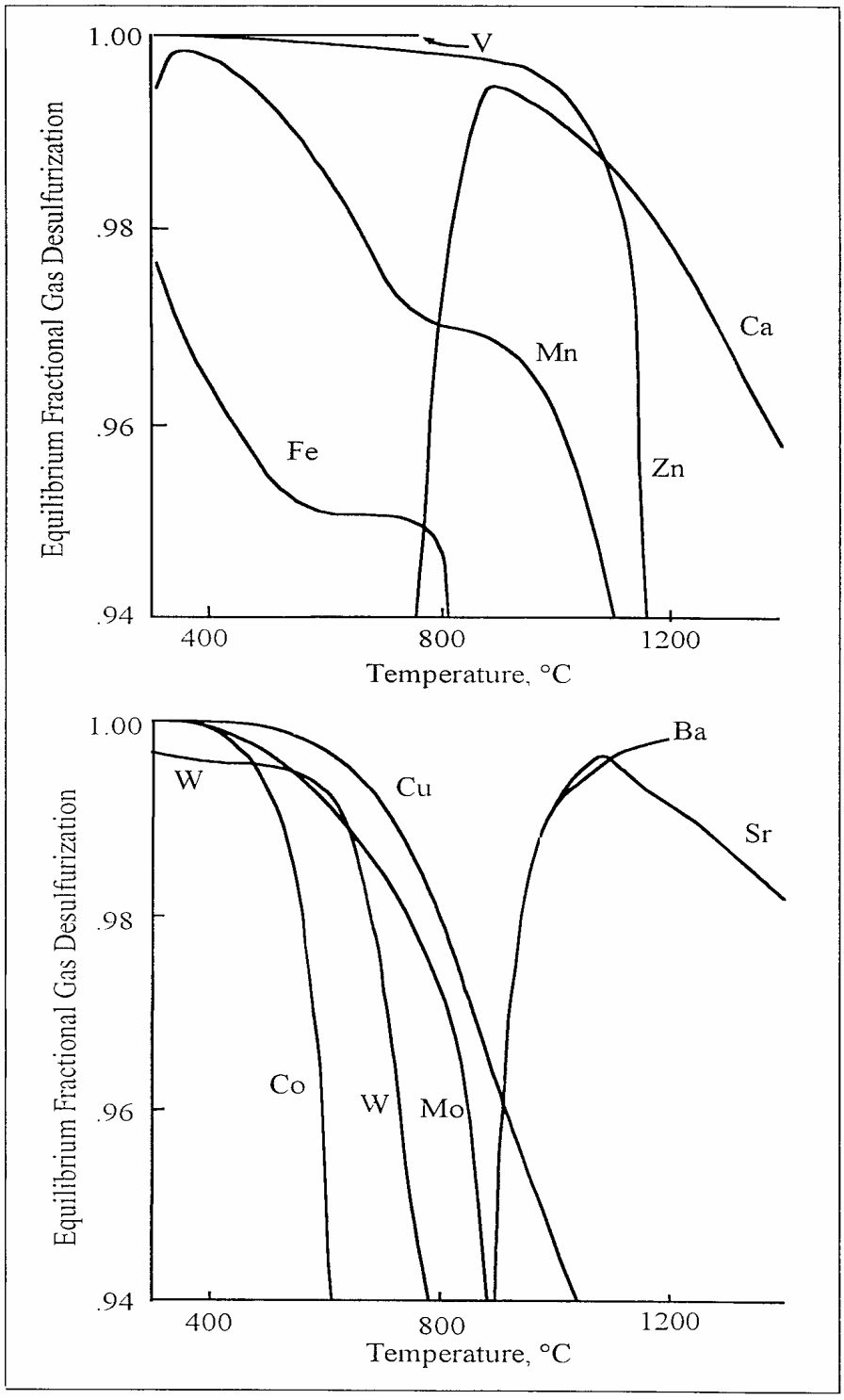

Figure 2.4 Desulfurization Potentials of Eleven Metals [25]

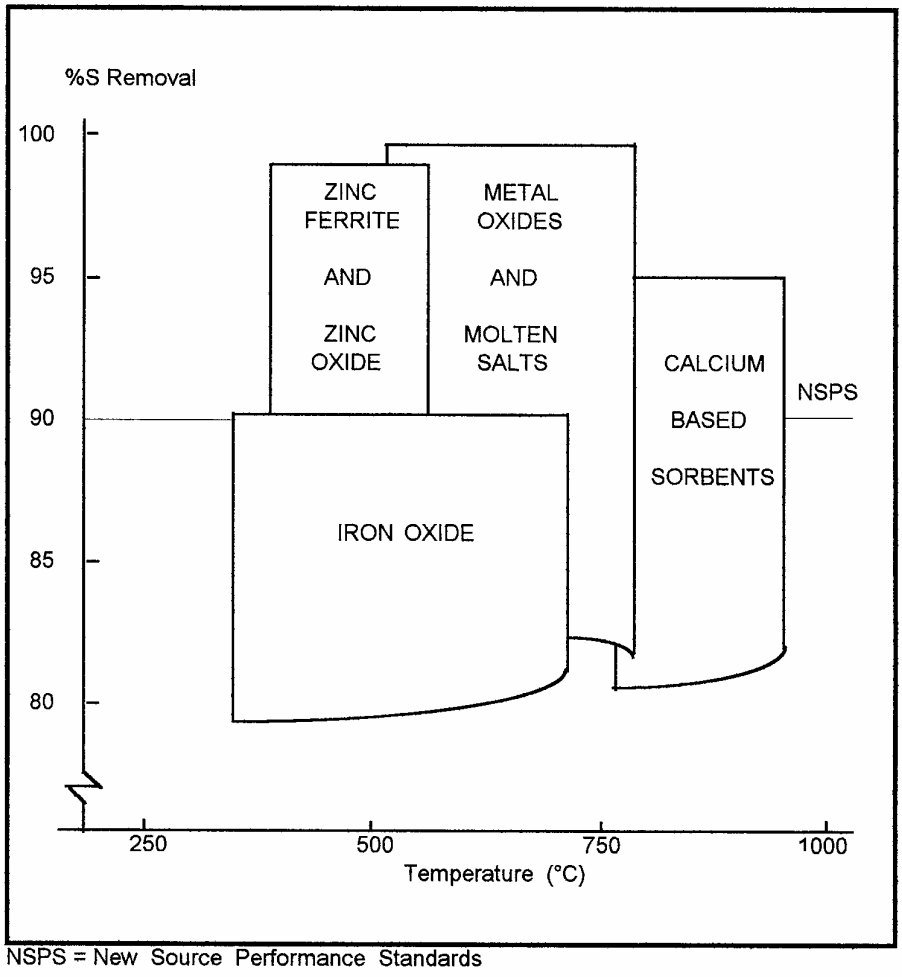

Figure 2.5 Sulfur Removal Efficiencies of Several Metal Oxides [19]

The choice of primary metal oxide for the sorbent depends on the temperature of interest and the degree of sulfur removal required. Formulations based on calcium, zinc, iron, copper, molybdenum, nickel, manganese and tin have been reported in the literature for use on coal gases in the temperature range 250°C to 900°C [1, 2, 3, 4, 10, 19, 21].

2.3.1.1.1 Iron Oxide

Because of its low cost and its earlier use for desulfurization of town gas, iron oxide was the first material to be examined as a regenerable sorbent for coal gas desulfurization [24].

The overall sulfidation and regeneration reactions are as follows:

Sulfidation:

$$Fe_2O_3 + 2H_2S + H_2 \longrightarrow 2FeS + 3H_2O \quad (2.1)$$

$$FeO + H_2S \longrightarrow FeS + H_2O \quad (2.2)$$

Regeneration:

$$2FeS + 7/2O_2 \longrightarrow Fe_2O_3 + 2SO_2 \quad (2.3)$$

Tamhankar et al. [27] observed two-stage reaction between iron oxide and hydrogen sulfide in his experiments with thermogravimetric analyzer (TGA) where they followed the change in weight of sorbents during the sulfidation in the temperature range of 600 – 800ºC. In the first stage iron oxide was reduced to iron metal and the second stage was the reaction of iron with hydrogen sulfide resulted in iron sulfide. It was reported that the sulfidation and reduction reactions were first order with respect to gas concentration and the rate was affected by H_2S concentration and particle size.

The H_2S equilibrium concentration over iron oxide rises rapidly at temperatures above 800ºK, thus, the possible removal efficiency becomes too low. Therefore, other sorbents, especially those based on zinc, were considered in the early 1980s. However, the opinion on the optimum temperature range

has been changed lately and desulfurization temperatures in the order of 600-800ºK are currently preferred because it is indicated that too high temperatures carry significant penalties in terms of the costs of construction materials. With respect to the optimum temperature range, a reasonable compromise between cycle efficiency, capital costs and operating costs, leads to values between 600ºK and 800ºK [28]. At that temperature level, iron oxide is again an attractive sorbent; apart from its high reactivity, it has the following obvious advantages [29]:

- cheap,
- non-toxic,
- high H_2S removal efficiency,
- easily regenerable.

The Appleby-Frodingham Process is the earliest known iron oxide process that has been commercialized. In this plant, the crude coke oven gas was passed through a fluidized-bed of sintered iron oxide powder, where up to 98% of the H_2S was removed by reaction with Fe_2O_3 [4].

The US Bureau of Mines [30] carried out laboratory testing of different solid sorbents, mainly containing some form of iron, in order to evaluate their performance for removal of H_2S from hot simulated producer gas. The results of these studies indicate that a broad range of iron-based sorbents is potentially suitable for removal of H_2S from coal gas streams at elevated temperatures.

In 1988, Focht et al. [31], has shown that Fe_3O_4 is significantly more reactive with H_2S than Fe and therefore, it follows that an iron-based sorbent is the most suitable for a low reducing power fuel gas. Moreover, iron based sorbents require low temperature for complete oxidative regeneration without sulfate

formation. Therefore, since regeneration of iron sulfide to iron oxide may be carried out at a lower temperature, the use of iron-based sorbent appears to be the best approach to achieve an energetically viable cyclic sulfidation/regeneration process in the temperature range of 350 – 550ºC [2].

The sulfate formation can be observed in the regeneration with air at temperatures below 480ºC, which reduces the H_2S removal capacity of the sorbent [32]. However, the iron oxide could be regenerated with SO_2 to directly convert the iron sulfide to elemental sulfur, further improving process economics at the moderate temperatures.

2.3.1.1.2 Zinc Oxide

Zinc based sorbents are potentially attractive for high temperature applications because of their favorable thermochemical properties. Zinc oxide is more stable in the reducing coal gas atmosphere than, for example, Fe_2O_3 or CuO, although reduction of ZnO to volatile elemental zinc vapor can occur at high temperature in highly reducing atmospheres [25].

The overall sulfidation and regeneration reactions of ZnO are as follows:

Sulfidation:

$$ZnO + H_2S \longrightarrow ZnS + H_2O \quad (2.4)$$

Regeneration:

$$ZnS + 3/2O_2 \longrightarrow ZnO + SO_2 \quad (2.5)$$

The regenerability of ZnO is restricted by loss of surface area (sintering) at high regeneration temperatures. Therefore, in order to overcome these drawbacks of ZnO, studies were carried out by combining the ZnO with other metal oxides.

The mixed oxide sorbent zinc ferrite, $ZnFe_2O_4$, combining ZnO with Fe_2O_3 was developed as an alternative to single zinc oxide sorbent because of its high sulfur capacity, rapid reaction with H_2S, and high H_2S removal efficiency [33]. In 1981, Grindley and Steinfield [34] studied with zinc ferrite in a fixed bed process development unit operated by KRW Energy Systems. The results have been generally favorable. $ZnFe_2O_4$ has a high sulfur capacity and reacts rapidly and completely with H_2S. Exit H_2S concentrations of approximately 5 ppmv have been achieved prior to breakthrough from fixed-bed test reactors [34]. The sulfided sorbent has been regenerated with air and steam and then resulfided without major reactivity losses.

However, zinc ferrite decomposes into ($ZnO+Fe_3O_4$) in the reducing coal gas atmosphere. Hence, it is similarly limited (as ZnO) to an operating temperature of approximately 600ºC [35].

It is reported that the addition of TiO_2 stabilized the ZnO, thereby permitting an increase in operating temperature. The stabilizing effect was attributed to the formation of mixed metal oxides compounds including $ZnTiO_3$, Zn_2TiO_4 and $Zn_2Ti_3O_8$. However, the increased stability is offset by reduced sulfur capacity since TiO_2 does not react with H_2S at the conditions of interest. The theoretical capacity (based on stoichiometry) of a sorbent containing equimolar quantities of ZnO and TiO_2 is 198 g of sulfur per kg of sorbent compared to 398 g of sulfur per kg of sorbent for $ZnFe_2O_4$ [1].

2.4 Industrial Wastes as Desulfurization Sorbent

An alternative approach is to develeop a more economical hot gas desulfurization system for IGCC processes that utilizes low-cost (or essentially free of charge) metal oxide-containing waste materials from metal processing, smelting, and refining operations. The number of cycles required for economic viability of the desulfurization process will be determined by the cost of sorbent production from the waste metal oxides. Therefore, given the low cost of these waste raw materials, a significant reduction in the cost of hot gas desulfurization can be realized, even if the sorbent can remain effective for only a relatively small number of sulfidation/regeneration cycles. The use/reuse of abundant waste materials contributes to energy and resource conservation. Additionally, no further treatment of the waste solids is required prior to disposal. There is also a potential for direct elemental sulfur production, which is more valuable than SO_2 [4].

It is investigated that waste slag from iron and steel industry is composed mainly of metal oxide, which can be used as desulfurization sorbent at elevated temperatures. This waste slag is deposited on the land causing environmental pollution. So, reusing of this waste slag in desulfurization process shall prevent environmental pollution while supplying a desulfurization sorbent almost free of charge. Also, metal oxides like ZnO and FeO are present in the waste slag from zinc industry and it may be utilized as desulfurization sorbent as steel slag.

Slimane and Abbasian [4] carried out a study by using metal oxide waste materials from metal processing operations in order to obtain the reactivities of these metal oxides toward H_2S in the temperature range of 400 – 600ºC. All metal oxide waste materials

performed quite well, achieving effective sulfur capacities of approximately 20 g S / 100 g material.

Sarıçiçek [3] carried out a study with the waste materials from iron-steel and zinc industries (steel slag and zinc slag, namely). In this study, inlet H_2S concentration range was 1000 – 2000 ppmv at the temperature range of 400 – 600ºC. The results of this study showed that zinc slag and steel slag can remove the H_2S effectively from the coal gas and they can be used as desulfurization sorbent .

2.4.1 Steel Slag

In Turkey, there are a few integrated iron and steel plants, which produce about 1.5-2 million tons of steel slag per year. KARDEMİR, one of the integrated iron and steel plants, has generated about 5 million tons of steel slag over the years.

In iron and steel production plant, firstly, iron is produced from iron ore in blast furnace. Then, steel is obtained by removing the impurities such as C, Si, Mn, S and P by oxidation from pig iron. Steel slag formation occurs in basic oxygen furnace together with steel. Steel slag is a hard and dense material. The high density and hardness of steel slag make it particularly suitable as road aggregate [36].

Steel slag is relatively non-porous and consequently makes a high-density stone of high crushing strength. The typical composition of steel slag analyzed at KARDEMİR laboratories is given in Table 2.2 [3].

Table 2.2 Chemical Composition of Steel Slag at KARDEMİR [3]

Composition	Weight %
FeO	10 – 36
SiO_2	13 – 30
MnO	6 – 16
Al_2O_3	2.5 – 3.5
CaO	22 – 45
MgO	2.5 – 14
S	-

From Table 2.2, it can be seen that steel slag is mainly composed of metal oxides FeO, CaO, and MnO. In the literature, these metal oxides were found to be very suitable for hot gas desulfurization. For this reason, it is decided to use steel slag in this study.

2.4.2 Zinc Slag

ÇİNKUR is the largest zinc production plant in Turkey. ÇİNKUR has stopped its operation and no zinc is produced in the plant since 5-6 years. However, the Waelz furnace slag produced previously has been piled in the plant area and the amount is on the order of million tons. The typical analysis of zinc slag from Waelz furnace is given in Table 2.3 [37].

Table 2.3 The Typical Analysis of Waelz Furnace Slag [37]

Components	Weight %
Zn	3.5
Fe	26.0
CaO	14.0
Al_2O_3	11.0
SiO_2	22.0
C	15.0

As can be seen from Table 2.3, zinc slag also contains the thermodynamically favorable metals, such as Zn and Fe, reported by Westmoreland and Harrison [25] for the desulfurization of hot coal gas.

2.5 Deactivation Model

The formation of a dense product layer over the solid reactant creates an additional diffusion resistance. This resistance may reduce the reaction rate. It would be expected that this result will cause significant changes in the pore structure, active surface area, and activity per unit area of solid reactant with the extent of reaction. All of these changes cause a decrease of activity of solid reactant with time [26].

In the literature, it is reported that the deactivation model works well for such gas–solid reactions. In this model, the effects of all of these factors on diminishing rate of sulfur fixation were combined in a deactivation rate term.

Yasyerli et al. [26] improved breakthrough equation in order to predict the breakthrough curves including the deactivation of sorbent in the calculations.

In the study carried out by Yasyerli et al. [26], the isothermal species conservation equation for the reactant gas H_2S in the packed column with the pseudo-steady-state assumption was taken as:

$$-Q\frac{dC_A}{dW} - k_0 C_A a = 0 \tag{2.6}$$

where C_A = concentration of reactant gas, kmol/m^3

W = sorbent mass, kg

Q = volumetric flowrate of gas, m^3/min

k_0 = initial sorption rate constant, m^3/kg.min

a = activity of the solid sorbent

In this equation, axial dispersion in the packed column and any mass transfer resistances were assumed to be negligible. According to the proposed deactivation model, the rate of change of the activity of the solid reactant (a) was expressed as:

$$-\frac{da}{dt} = k_d C_A{}^n a^m \tag{2.7}$$

where k_d is the deactivation rate constant, and n and m are exponential coefficients.

In order to obtain the zeroth solution of the deactivation model, n = 0, m = 1 were taken and the initial activity of the solid was assumed to be unity. The solution of Eq. (2.6) is given as:

$$C_A = C_{A0} \exp\left[-\frac{k_0 W}{Q} \exp(-k_d t) \right] \tag{2.8}$$

where C_{A0} is the initial concentration of reactant gas. This solution of the first equation is equivalent to the breakthrough equation proposed by Suyadal et al. [38] and assumes a fluid phase concentration that is independent of deactivation processes along the reactor. As a matter of the fact, the deactivation rate depends on the concentration and, accordingly, on the axial position in the packed bed.

Furthermore, Yasyerli et al. [26] applied an iterative procedure in order to obtain analytical solutions of Eqs. (2.6) and (2.7) by taking n = m = 1. The procedure used here was similar to the procedure for the approximate solution of nonlinear equations, proposed by Doğu [39]. In this procedure, the zeroth solution (Eq. (2.8)) was substituted into Eq. (2.7), and the first correction for the activity was obtained by the integration of this equation. Then, the corrected activity (a) expression was substituted into Eq. (2.6), and integration of this equation gave the first corrected solution for the breakthrough curve.

$$\frac{C_A}{C_{A0}} = \exp\left\{\frac{\left[1-\exp\left(\frac{k_0 W}{Q}\left(1-\exp\left(-k_d t\right)\right)\right)\right]}{\left[1-\exp\left(-k_d t\right)\right]}\exp\left(-k_d t\right)\right\} \tag{2.9}$$

This iterative procedure could be repeated for further improvement of the solution. In this procedure, higher order terms in the series solutions of the integrals were neglected [26].

CHAPTER 3

EXPERIMENTAL SECTION

3.1 Sorbent Properties

The sorbents used in this study were characterized before in a previous study done by Sarıçiçek [3]. Since the same samples were used in this study, the characterization of samples were not repeated again, and the data from Sarıçiçek [3] were used.

3.1.1 Physical Characterization of the Sorbent

BET surface area analysis and mercury intrusion porosimetry analysis were determined by Sarıçiçek [3] for both slags by using Micromeritics ASAP 2000. Porosity of particles and pore size distribution were analyzed by Micromeritics Pore Sizer 9310, Mercury porosimetry [3].

The physical alterations in the sorbents were also determined by Sarıçiçek [3] by using scanning electron microscope (SEM) in the Department of Metallurgical and Materials Engineering before and after sulfidation experiments. The instrument used was a "Jeol JSM-6400 Scanning Electron Microscope".

3.1.1.1 Steel Slag

Since the same samples of steel slag that Sarıçiçek [3] has used were tested in this study, the results of the BET surface area analysis and mercury intrusion porosimetry analysis were taken from Sarıçiçek [3]. Table 3.1 shows the BET surface areas of steel slag [3]. The maximum BET surface area belongs to the particle size of 2-3 mm for steel slag.

Table 3.1 BET Surface Areas of Fresh Steel Slag [3]

	Sorbent Particle Size, mm	BET Surface Area (m^2/g)
Steel Slag	1-2	1.54
	2-3	3.10
	3-4	2.93

In Table 3.2, mercury porosimetry analysis of fresh (unused) steel slag is given [3]. As can be seen from the table, the total pore volume is about 0.008, 0.034, and 0.004 cm^3/g for the particle sizes of 1-2 mm, 2-3 mm, and 3-4 mm, respectively. The highest pore volume belongs to 2-3 mm steel slag. Again,

steel slag having particle size of 2-3 mm in diameter has the highest porosity among the other particle sizes.

Table 3.2 Mercury Porosimetry Analysis of Steel Slag [3]

	Steel Slag 2 – 3 mm
Average pore diameter (μm)	0.0521
Total pore volume (cm^3/g)	0.0340
Total Pore Area (m^2/g)	2.6105
Bulk Density (g/cm^3)	3.4981
Porosity (%)	11.89

The mercury porosimetry profiles of 2-3 mm particles of steel slag were obtained by Sarıçiçek [3] previously and are given in Figure 3.1 and 3.2 [3]. Figure 3.1 shows that the pore diameters of 2-3 mm particles change between 3 μm and 37 μm with a cumulative intrusion volume of 0.004 cm^3/g. There are pores around 1-2 μm and the total intrusion volume is about 0.012 cm^3/g. Figure 3.2 gives the incremental intrusion volumes of 2-3 mm steel slag. Again, Figure 3.2 shows a biomodal distribution in pore structure [3].

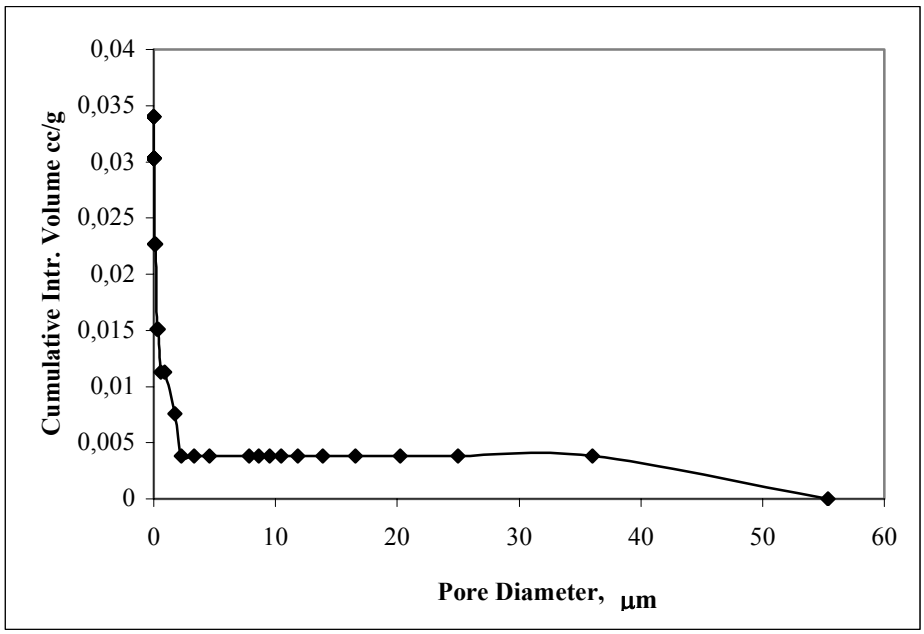

Figure 3.1 Cumulative Pore Distributions of 2-3 mm Steel Slag [3]

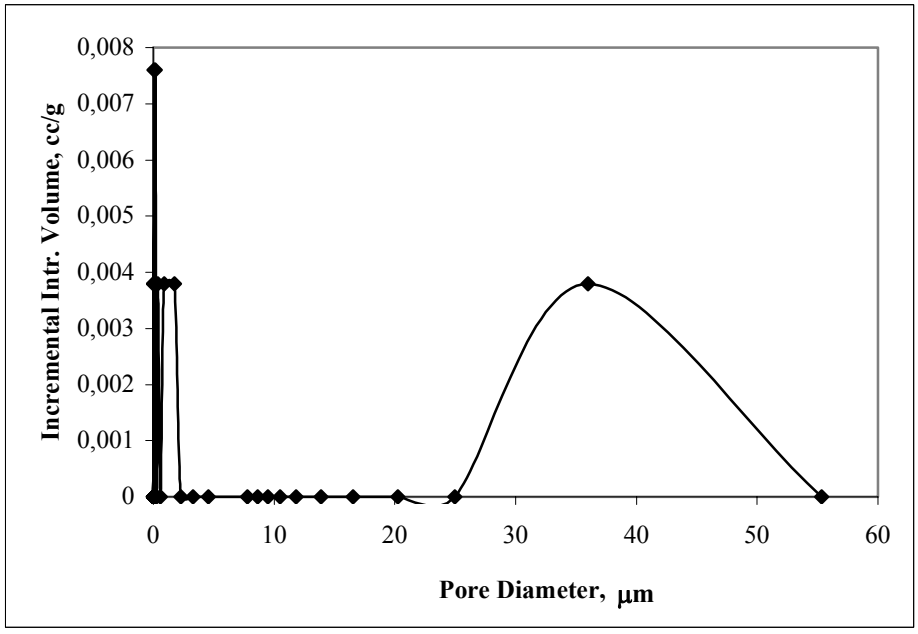

Figure 3.2 Incremental Intrusion Volumes of 2-3 mm Steel Slag [3]

SEM photographs of 2-3 mm steel slag are given in Figure 3.3 [3]. From figure, it can be seen that steel slag has a complex structure and there are mainly crystalline and rod shapped structures. The structure is very porous. There are some pores which are larger than 300 μm in diameter. The crystals are due to calcium silicates and calcium iron silicates [3].

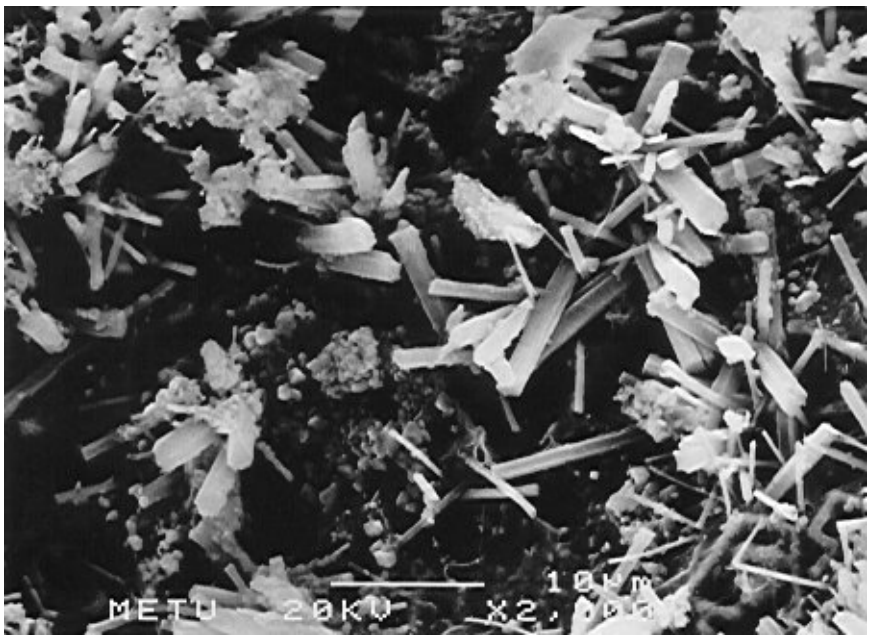

Figure 3.3a SEM Photographs of 2-3 mm Fresh Steel Slag (x2000) [3]

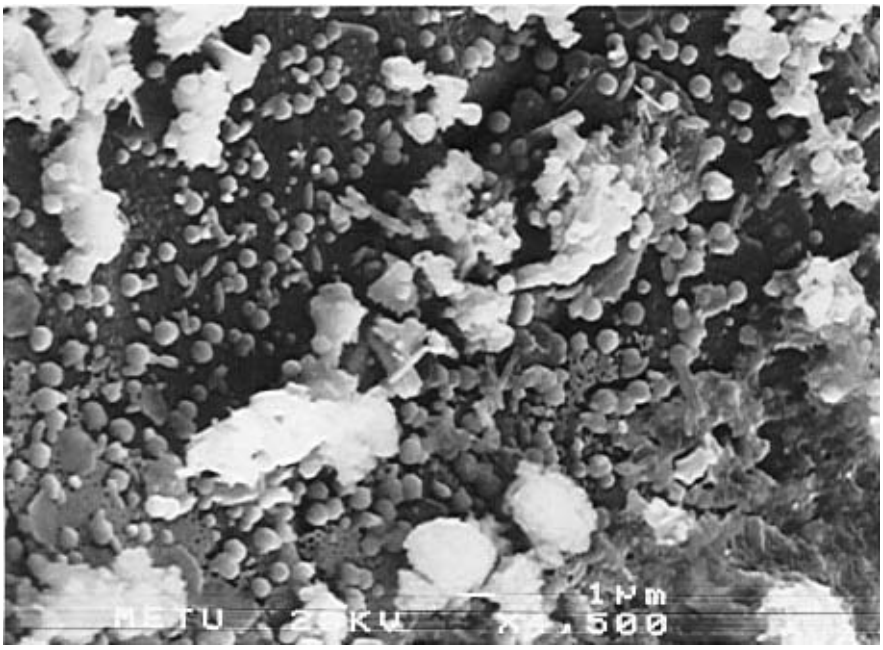

Figure 3.3b SEM Photographs of 2-3 mm Fresh Steel Slag (x4500) [3]

3.1.1.2 Zinc Slag

Sarıçiçek [3] has reported the BET surface area for 2-3 mm zinc slag as 3.14 m^2/g, which is higher than BET surface area of steel slag.

Mercury porosimetry analysis of fresh (unused) zinc slag is given in Table 3.3 [3]. According to the table, the porosity of the 2-3 mm zinc slag, which is 0.3152, is higher than the porosity of the 2-3 mm steel slag, which is 0.1189. That is, fresh zinc slag has more porous structure than steel slag.

Table 3.3 Mercury Porosimetry Analysis of Fresh Zinc Slag [3]

	Zinc Slag
	2-3 mm
Average pore diameter (μm)	0.2403
Total pore volume (cm^3/g)	0.6235
Total Pore Area (m^2/g)	10.3791
Bulk Density (g/cm^3)	1.3116
Porosity (%)	31.52

The mercury porosimetry profiles of 2-3 mm particles of zinc slag are given in Figure 3.4 [3]. Figure 3.4 shows that the pore diameters change between 1 μm and 55 μm with a cumulative intrusion volume varying between 0.6 and 0.2 cm^3/g. Figure 3.5 gives the incremental intrusion volumes.

SEM photographs of 2-3 mm zinc slag are given in Figure 3.6 [3]. From figure, it can be seen that the morphological structure of the zinc slag is less crystalline and rod shapped crystals are not common as compared to steel slag.

3.1.2 Chemical Characterization of the Sorbent

The metal oxide content of the steel slag from KARDEMİR was analyzed in the laboratory of KARDEMİR with X-Ray Spectrophotometer. The metal analyses of zinc slag obtained from ÇİNKUR were done by using Atomic Absorption Spectrophotometer [3].

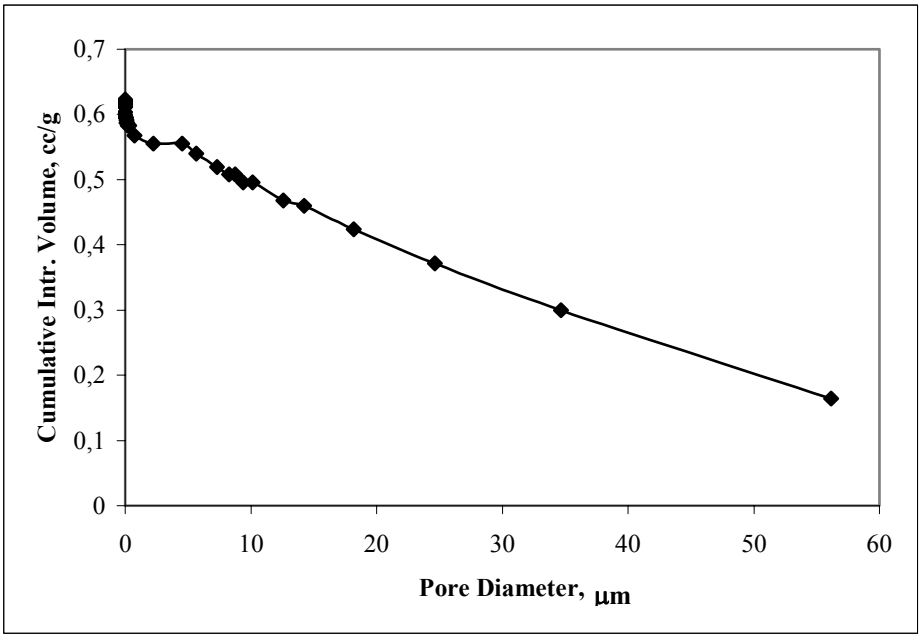

Figure 3.4 Cumulative Pore Distributions of 2-3 mm Zinc Slag [3]

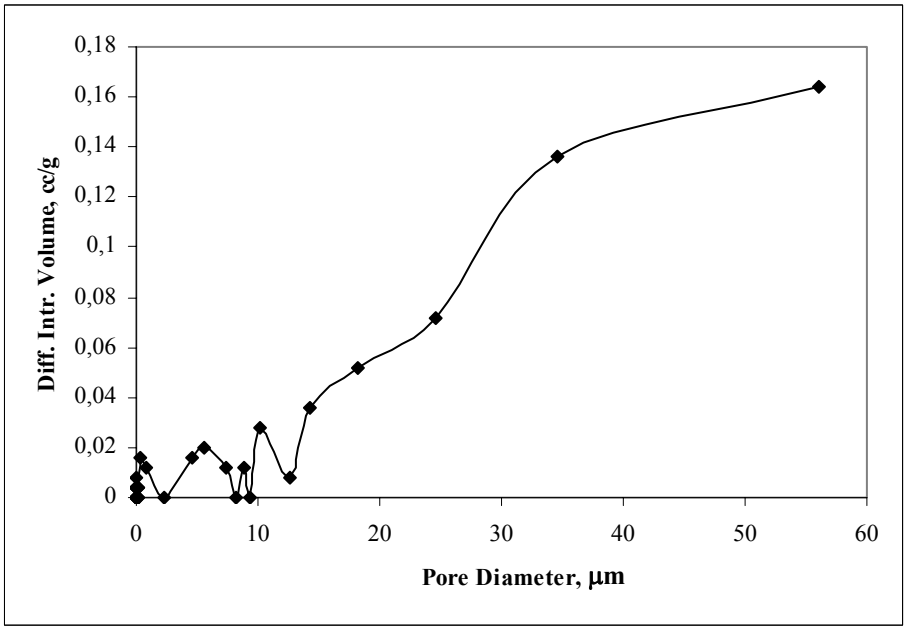

Figure 3.5 Differential Intrusion Volumes of 2-3 mm Zinc Slag [3]

Figure 3.6a SEM Photographs of 2-3 mm Zinc Slag [3]
(x3500)

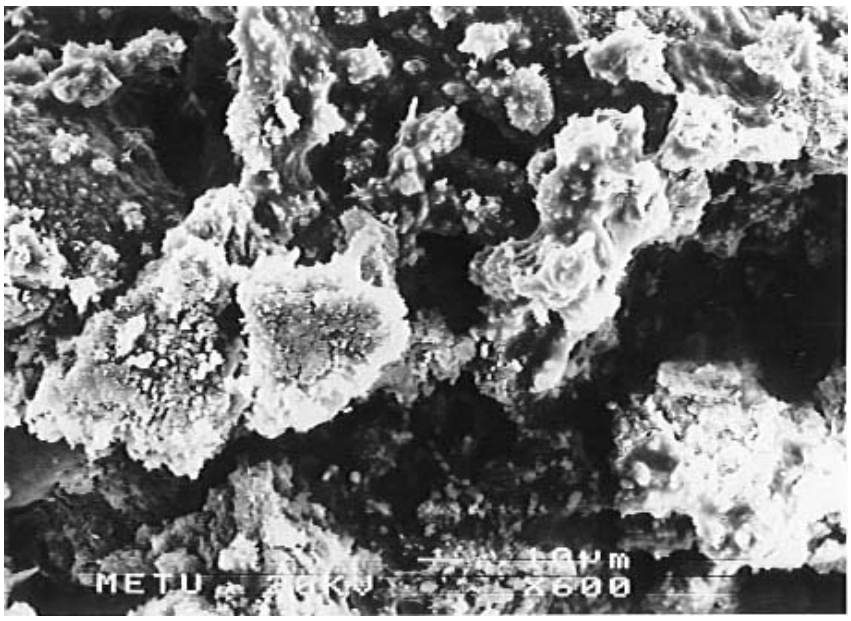

Figure 3.6b SEM Photographs of 2-3 mm Zinc Slag [3]
(x600)

For detection of the crystalline structure of the sorbent before sulfidation and the different phases contained by the sorbent after sulfidation, X-Ray Diffraction analyses were performed with Philips X-Ray Diffractometer in the Department of Metallurgical and Materials Engineering at METU.

3.1.2.1 Steel Slag

The samples used in this study are the same as the samples used in the previous study [3]. Therefore, the chemical characterization of samples are taken from Sarıçiçek [3]. Chemical analysis of steel slag was performed by X-Ray spectrometry in the laboratories of KARDEMİR and the results of the analysis for 2-3 mm particles are given in Table 3.4 [3]. From the table, it can be seen that steel slag is composed of mainly Fe, Ca and Si oxides. Oxides of Fe, Mn and Ca are some of the most favorable desulfurization sorbents [25].

Table 3.4 Chemical Analysis of Steel Slag (% by wt.) [3]

%	2 – 3 mm
Fe	16.80
Si	8.27
Mn	5.04
Al	1.13
Ca	24.02
Mg	4.65

XRD analysis of steel slag obtained from the previous study [3] is given in Figure 3.7. $CaFeSiO_4$, FeO, CaO and $2CaO.SiO_2$ are the most commonly found phases present in the fresh steel slag [3].

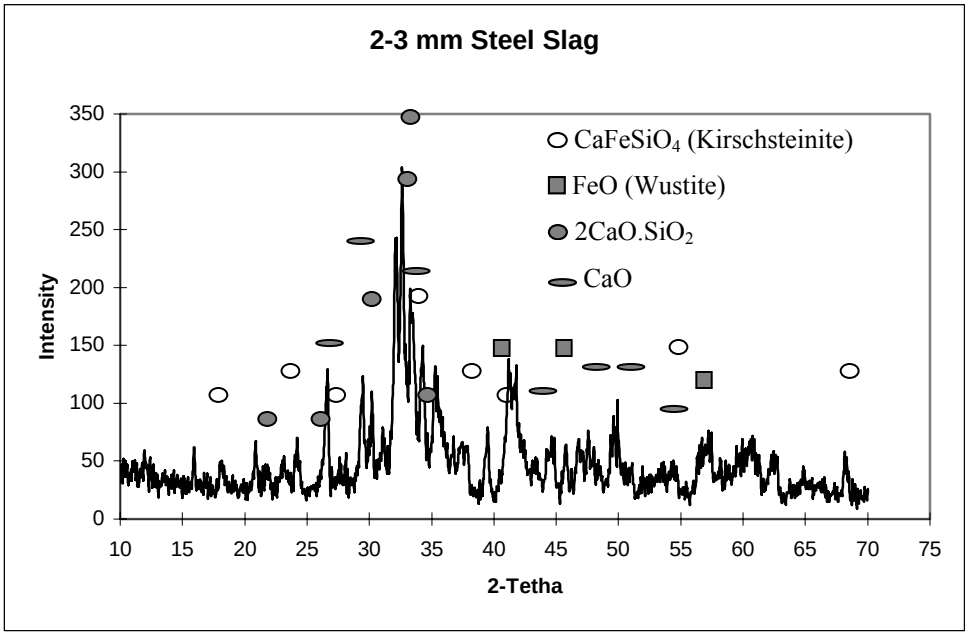

Figure 3.7 XRD Analyses of 2-3 mm Fresh Steel Slag [3]

3.1.2.2 Zinc Slag

The results of chemical analysis of zinc slag determined by AAS are given in Table 3.5 as reported by Sarıçiçek [3]. The zinc slag composition is also rich in the metals that are proved to have high sulfur capacity. Therefore, zinc slag is a strong candidate for removing H_2S. Also, Fe and Zn in the zinc slag can behave like zinc ferrite sorbent which is a very efficient sorbent for H_2S.

Table 3.5 Chemical Analysis of Zinc Slag [3]

	% by wt
Zn	1.70
Fe	8.28
Ca	11.03
Mn	0.60

The XRD analyses of zinc slag, given in Figure 3.8, shows that Fe, $Ca_2Al_2SiO_7$, and $Ca_2ZnSi_2O_7$ are present in the fresh zinc slag sorbent [3].

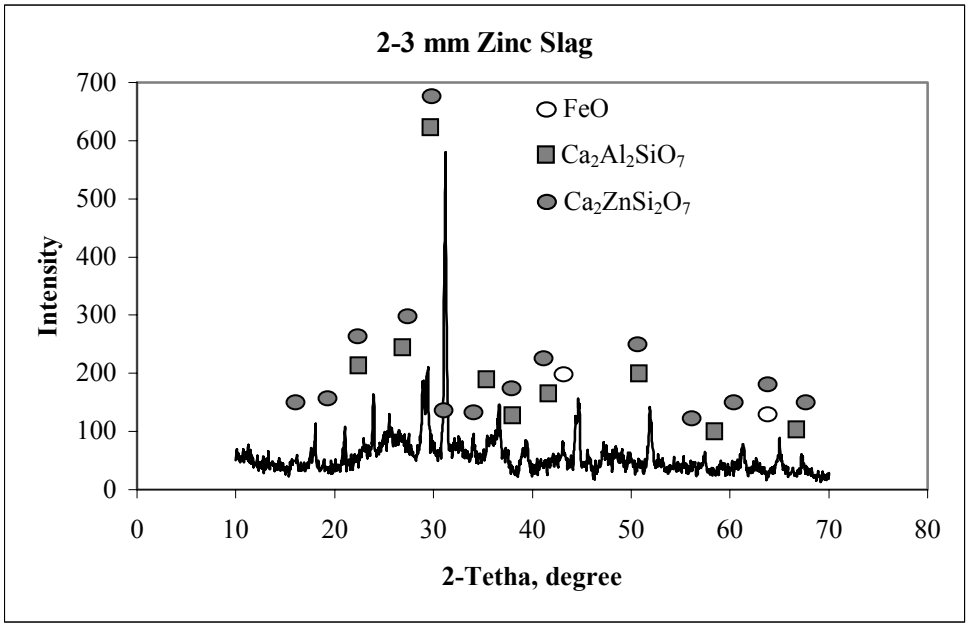

Figure 3.8 XRD Analyses of 2-3 mm Zinc Slag [3]

3.2 Experimental Setup

The same experimental setup was used in this study as it was in the study of Sarıçiçek [3]. Experimental setup for desulfurization of coal gas includes three parts: gas suppliers, flow controllers and reactor-furnace system. The schematic diagram of the experimental setup is given in Figure 3.9.

Coal gas contains CO, CH_4, H_2, N_2, H_2O, and H_2S. However, preparation of the coal gas with these components is difficult in the laboratory conditions. Therefore, simulated reactive gas mixture was prepared in this study and contains varying amounts of H_2S, N_2 and H_2. The purities of gases used were as follows:

- H_2S: 99.5 %
- N_2: 99.999 %
- H_2: 99.0 %

A mixture of H_2S, N_2 and H_2 was supplied to the reactor from compressed gas cylinders.

The flowrates of H_2S, N_2 and H_2 gases are regulated by using flow controllers on the control panel. After necessary adjustment of each gas is made for desulfurization experiments, these gases are mixed in a manifold behind the control panel and the mixture becomes ready for entering the reactor. In addition, three-way valves are placed before the reactor in order to allow the gas mixture through the bypass line during flow rate adjustments.

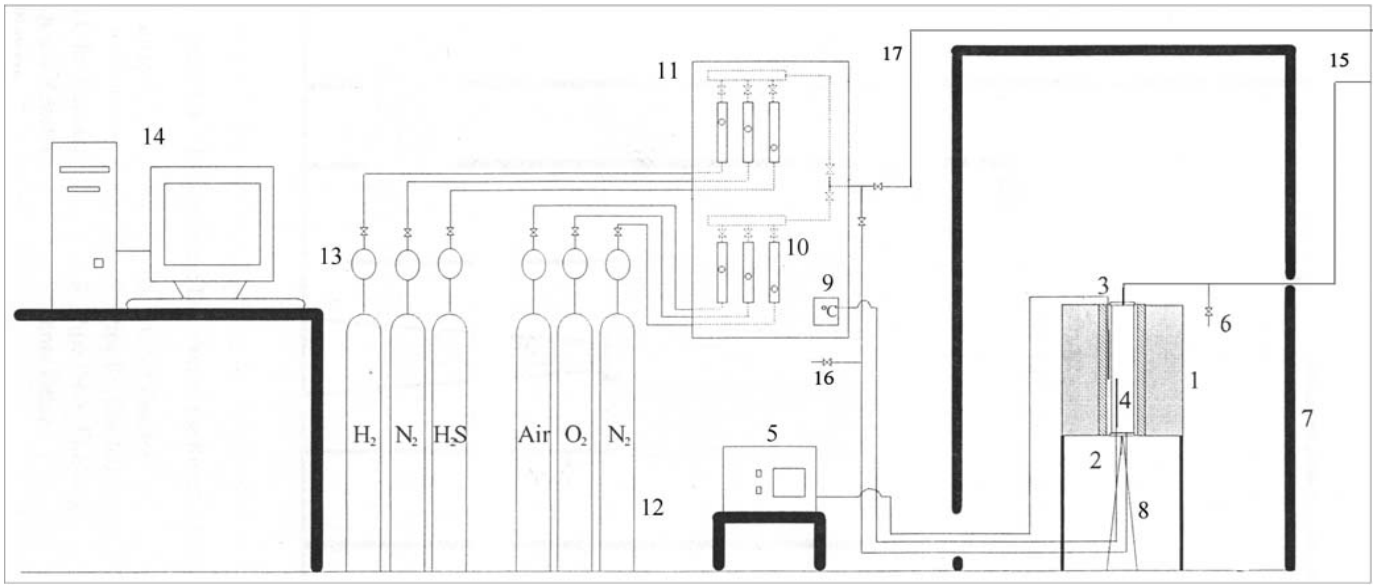

Figure 3.9 Schematic Diagram of Experimental Setup [3]

1. Furnace
2. Thermocouple for Reactor
3. Thermocouple for Furnace
4. Reactor
5. Furnace Control
6. Outlet Gas Sampling Port
7. Cabin
8. Reactor Inlet Tubing
9. Temperature Display
10. Flowmeters
11. Control Panel
12. Gas Cylinders
13. Regulators
14. GC and Computer
15. Exhaust Fan
16. Inlet Gas Sampling Port
17. By-pass line

Reactor-furnace system consists of a quartz packed bed reactor and a tubular electrical furnace. The temperature of the furnace is adjusted by temperature control unit on the control panel. Reactor of 25-mm inner diameter and 760 mm long is placed vertically in the electrical furnace. Reactor made of quartz is used because of inertness and durability of the quartz to high temperatures. A porous quartz frit is also placed at the center of the reactor in order to support the sorbents and provide the inlet gas pass through from the bottom to the top of the reactor. The temperature in the reactor is controlled by a K-α type (Ni-Cr-Ni) thermocouple inside the reactor and it is connected to a digital display on the control panel. The temperature on this digital display is assumed as reaction temperature. For safety purposes, there is a plexiglas cabin surrounding reactor-furnace system. Exit gas from the top of the reactor is carried with a pipe which provides the connection between cabin and exhaust fan.

All fittings are connected with teflon tubings and stainless steel valves and joints are used in order to eliminate H_2S corrosion on the metal surfaces.

A VARIAN CP-3800 Gas Chromatograph with Pulsed Flame Photometric Detector (PFPD) is used for measuring the inlet and outlet concentrations of H_2S. The properties of the GC and the method used and the calibration curves are given in Appendix A.

3.3 Experimental Procedure

Sulfidation and regeneration experiments were conducted in order to have breakthrough curves for different metal oxide sorbents, various H_2S concentrations and temperatures. The reaction pressure was atmospheric in the

reactor. Reaction temperature during sulfidation and regeneration experiments was held constant.

Approximately 15 g of sorbent (about 12 cm^3 in volume) was put onto the quartz frit at the center of the reactor for each experiment. The bed height in the reactor was adjusted to 25 mm so that the diameter to height ratio was 1 for each experiment. Thus, in order to make every sorbent batch 25 mm in height for each experiment, the void volume between the particles of the sorbent was tried to be kept constant. After placing the sorbent onto the frit in the reactor, the furnace was allowed to be heated to the desired reaction temperature. Meanwhile, nitrogen gas was passed through the reactor in order to provide an inert environment. While the furnace was heated to the desired temperature, the simulated reactant gas mixture was prepared by using flow controllers. In this condition, three-way valve was open to the bypass line. During the adjustment of H_2S concentration, gas samples were taken at the inlet port of the reactor and H_2S concentration was measured on the GC. After the desired inlet H_2S concentration in the mixture was adjusted, the three-way valve was opened to the reactor and simulated gas mixture was passed through the reactor from bottom to top. Therefore, at this moment the experiment was started and the time t=0 was recorded.

During the sulfidation experiments, the samples were taken at 10 min intervals at the outlet port of the reactor by a gas-tight syringe. The gas samples were analyzed for exit H_2S (hydrogen sulfide) and COS (carbonyl sulfide) concentration in the Gas Chromatograph and breakthrough curves were obtained. However, no COS was detected in any of the outlet gas analyzed.

During the regeneration experiments, the outlet gas samples were analyzed for SO_2 in the GC.

3.3.1 Sulfidation Experiments

The basic reaction occurring during sulfidation experiments is the reaction of H_2S and the reactive metal oxide producing metal sulfide and water vapor.

$$M_yO_x + xH_2S \rightarrow M_yS_x + xH_2O \quad (3.1)$$

In this study, steel slag and zinc slag were chosen because they contain thermodynamically highly favorable metal oxides such as FeO and ZnO to react with H_2S. The particle size of 2-3 mm was studied for both steel slag and zinc slag. The reaction temperatures were in the range of 500-700ºC. The sulfidation experiments were carried out with inlet H_2S concentrations of 3000 ppmv, 4000 ppmv and 5000 ppmv. 10% by volume H_2 was added to inlet reactive gas mixture in order not to decompose H_2S in the gas mixture at the elevated temperatures. Remaining percentage apart from H_2S and H_2 in the mixture belonged to N_2. Total volumetric flowrate of gas mixture was adjusted to 204.17 ml/min (@25ºC, 1 atm) so that the space velocity in the reactor was 1000 hr^{-1} (@25ºC, 1 atm). The inlet gas compositions and flow rates used in the sulfidation experiments are given in Table 3.6.

Table 3.6 Inlet Gas Compositions for Sulfidation Experiments

H_2S concentration (ppmv)	H_2S (% by volume)	H_2 (% by volume)	N_2 (% by volume)
3000	0.3	10	89.7
4000	0.4	10	89.6
5000	0.5	10	89.5

In 2002, Sarıçiçek [3] conducted many sulfidation and regeneration experiments with steel slag, zinc slag and mixture of steel and zinc slag. However, the temperature range that he studied was 400-600ºC and the inlet H_2S concentrations were 1000 ppmv and 2000 ppmv. Total volumetric flowrate was 333 ml/min so that space velocity was 2000 hr^{-1}. As a matter of fact, this study is the continuation of the previous study.

3.3.2 Regeneration Experiments and Cyclic Tests

Regeneration is the reaction between metal sulfide and oxygen producing metal oxide again and SO_2.

$$M_yS_x + (3x/2)O_2 \rightarrow M_yO_x + xSO_2 \qquad (3.2)$$

Regenerability is an important factor in deciding the usage of metal oxides as desulfurization sorbent. Therefore, regeneration experiments are also carried out with steel slag and zinc slag.

The use of O_2-N_2 mixtures as regenerative gas leads to the production of dilute SO_2-containing gas streams and they can be converted to elemental sulfur or sulfuric acid by additional processes.

Regeneration temperature was kept the same as sulfidation temperature. Dry air was used as regenerative gas mixture. Thus, oxygen concentration in regenerative gas mixture was 21% by volume. Total volumetric flowrate of gas mixture was 210 ml/min. Three and a half successive cycles were applied to the sorbent. One cycle consisted of one successive sulfidation and regeneration experiment.

CHAPTER 4

RESULTS AND DISCUSSION

4.1 Sulfidation Experiments

Sulfidation experiments are carried out in order to determine the effects of temperature and inlet H_2S concentration on the sorption capacity of the desulfurization sorbents. Breakthrough curves are obtained by plotting exit H_2S concentration vs. reaction time. The exit H_2S concentration (C) was divided by inlet H_2S concentration (C_0) to provide dimensionless ordinate for all breakthrough curves in the sulfidation experiments. Thus, C/C_0 vs. time curves, where C is the exit H_2S concentration and C_0 is the inlet H_2S concentration, were plotted for each sulfidation run. Sorption capacities of the sorbent were calculated by using these breakthrough curves. Calculation of sorption capacities is given in Appendix B. The breakthrough concentration has been defined as 200 ppmv exit H_2S concentration since the gas turbines and other equipments in IGCC system can tolerate H_2S concentrations up to 150-200 ppmv [20].

In this study, replication experiments of the experiments done by Sarıçiçek [3] were conducted at the temperature range of 400 – 600ºC with 1000 ppmv and 2000 ppmv inlet H_2S concentrations and very similar results with the previous study were obtained.

4.1.1 Sulfidation Experiments with Steel Slag

Sulfidation experiments were carried out with steel slag at the temperatures of 500°C, 600°C and 700°C with 3000 ppmv, 4000 ppmv and 5000 ppmv inlet H_2S concentrations. In all sulfidation experiments, steel slag having 2-3 mm particle size was used. This was the same particle size that Sarıçiçek [3] has used and he worked with 1000 ppmv and 2000 ppmv inlet H_2S concentrations at the same temperatures mentioned above.

Breakthrough curves for H_2S obtained from the sulfidation experiments at 500°C, 600°C and 700°C with 3000 ppmv inlet H_2S concentration are given in Figure 4.1. As can be seen from Figure 4.1, H_2S sorption capacity of steel slag increases with increasing temperature. Also, 200-ppmv breakthrough concentration of H_2S is reached in about 15 min, 65 min and 125 min at temperatures of 500°C, 600°C and 700°C, respectively. No exit H_2S concentration can be observed from the reactor for 10 min, 30 min and 100 min at 500°C, 600°C and 700°C, respectively.

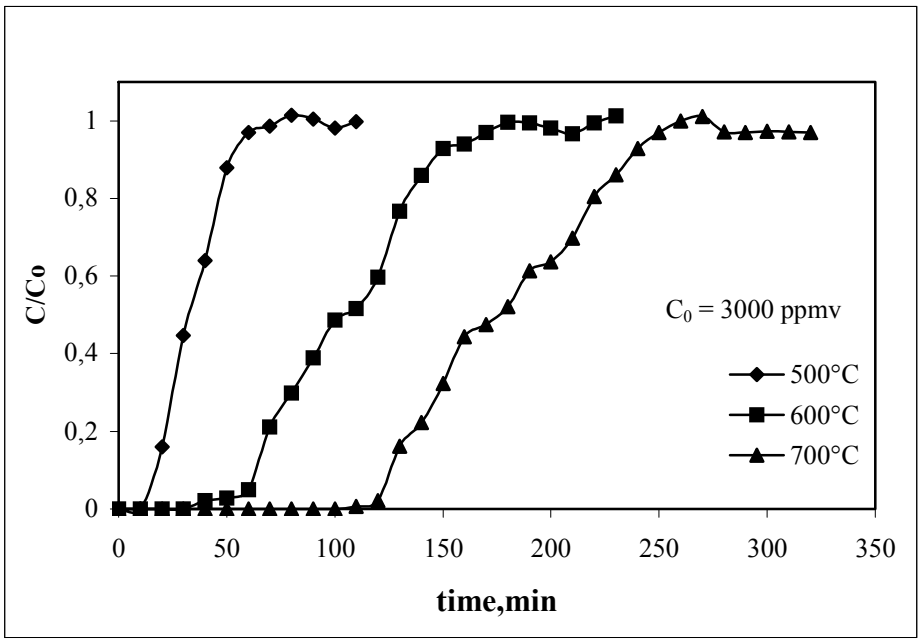

Figure 4.1 Breakthrough Curves for H_2S at Different Temperatures with 3000 ppmv Inlet Concentration (steel slag as sorbent)

Figure 4.2 indicates breakthrough curves for H_2S obtained from the sulfidation experiments carried out at reaction temperatures of 500, 600 and 700°C with 4000 ppmv inlet H_2S concentration. From Figure 4.2, it is seen that H_2S sorption capacity of the sorbent increases again with increasing temperature. 200 ppmv breakthrough concentration of H_2S is reached in about in 8 min, 25 min and 80 min for the temperatures of 500°C, 600°C and 700°C, respectively. The time intervals with no exit H_2S concentration are 0 min, 20 min and 70 min at temperatures of 500°C, 600°C and 700°C, respectively.

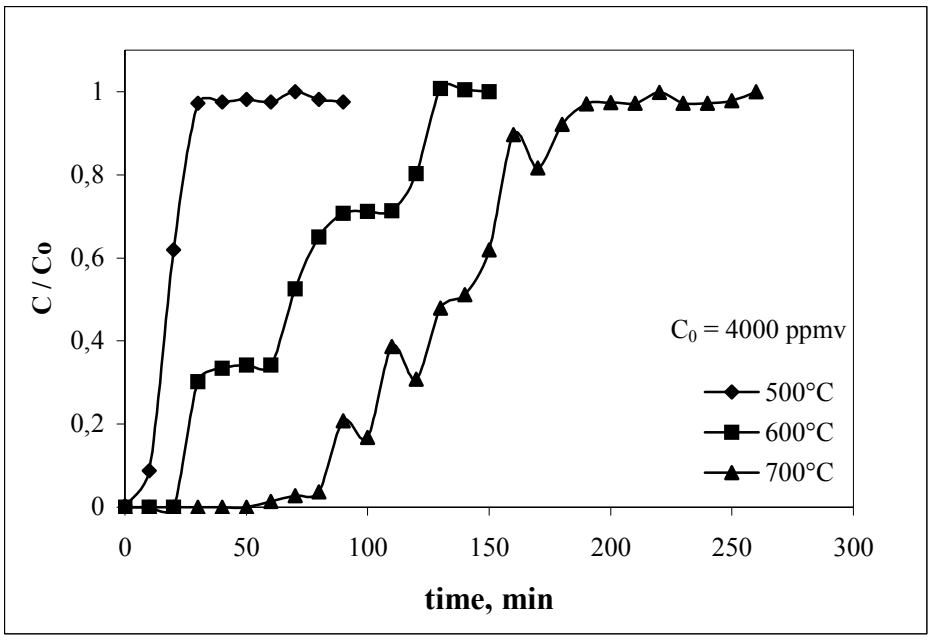

Figure 4.2 Breakthrough Curves for H_2S at Different Temperatures with 4000 ppmv Inlet Concentration (steel slag as sorbent)

Breakthrough curves for H_2S obtained again from the sulfidation experiments at reaction temperatures of 500, 600 and 700°C with 5000 ppmv inlet H_2S concentration are given in Figure 4.3. As it can be seen from Figure 4.3, H_2S sorption capacity of the sorbent increases with the increasing temperature as in the previous cases. 200-ppmv breakthrough concentration of H_2S is obtained immediately after the experiment starts at 500°C. At 600°C and 700°C, breakthrough concentrations are reached in about 5 min and 50 min, respectively. The time interval with zero H_2S concentration at the outlet gas reduces significantly for 5000 ppmv-inlet H_2S concentration.

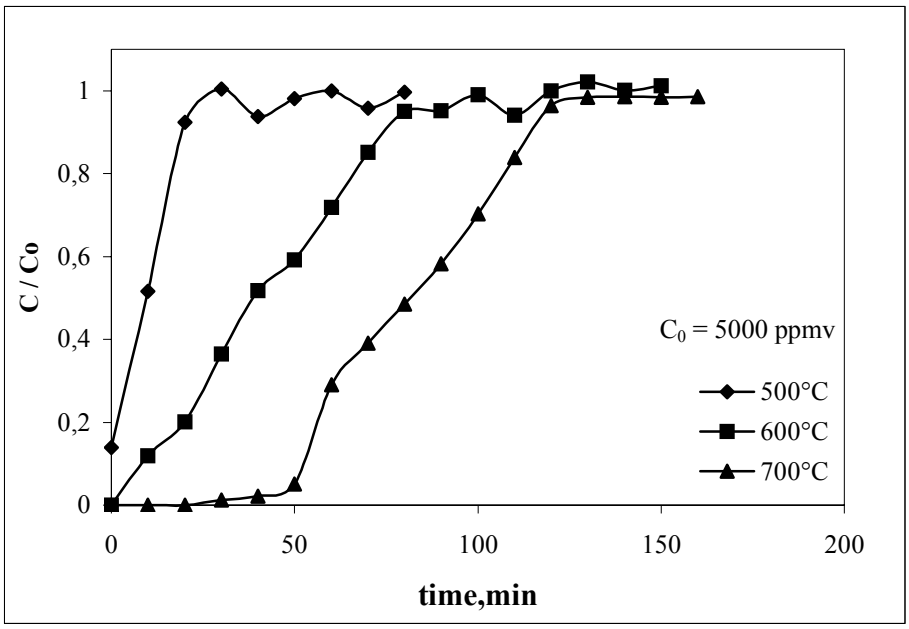

Figure 4.3 Breakthrough Curves for H_2S at Different Temperatures with 5000 ppmv Inlet Concentration (steel slag as sorbent)

From Figure 4.4, the effect of inlet H_2S concentration on the sorption capacity of the sorbent can be observed. Breakthrough curves obtained at the reaction temperature of 700°C with 3000, 4000 and 5000 ppmv inlet H_2S concentrations are given in the figure. The time interval with no H_2S concentration is about 20 min for 5000 ppmv inlet H_2S concentration while it is about 100 min for 3000 ppmv inlet H_2S concentration. It is obvious that the sorption capacity of the sorbent decreases with increasing inlet H_2S concentration. The amount of sorbent used in the experiments was 15 g.

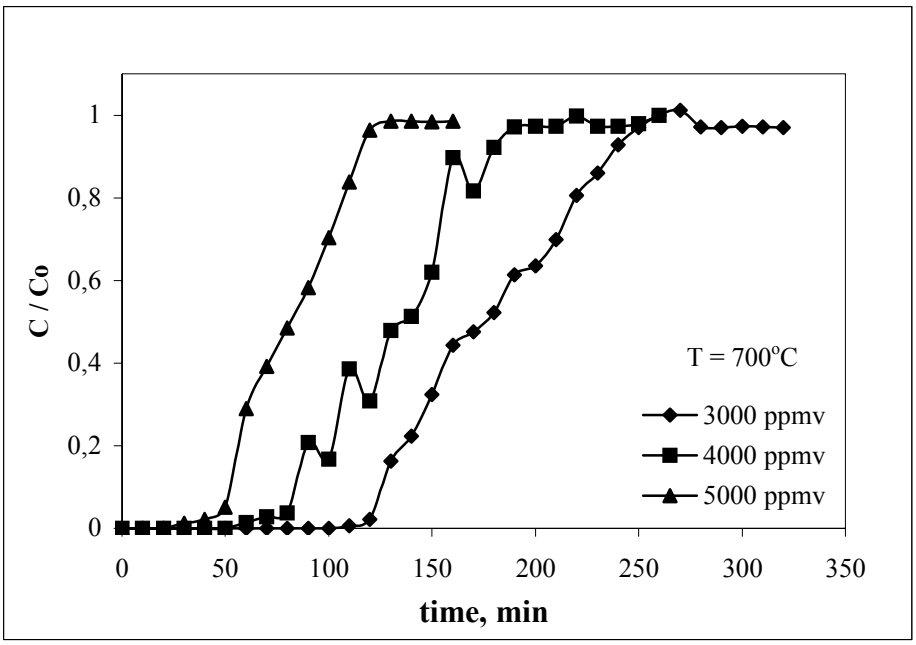

Figure 4.4 Breakthrough Curves for H_2S at 700°C Showing the Effect of Inlet Concentration (steel slag as sorbent)

As discussed earlier, Sarıçiçek [3] has done a series of sulfidation and regeneration experiments with both steel and zinc slags. He adjusted the inlet H_2S concentration to 1000 ppmv and 2000 ppmv and he carried out the experiments at the reaction temperatures of 400, 500 and 600°C. The comparison of the results of his experiments with those done with 3000, 4000 and 5000 ppmv at the temperatures of 500°C and 600°C will be discussed in this section.

Figure 4.5 shows the breakthrough curves obtained for 1000, 2000, 3000, 4000 and 5000 ppmv inlet H_2S concentrations at the reaction temperature of 500°C. This figure indicates the effect of the inlet H_2S concentration at the reaction temperature of 500°C. As can be seen from Figure 4.5, the sorption capacity of

the sorbent decreases with increasing inlet H_2S concentration including 1000 ppmv and 2000 ppmv. The sorption capacity of steel slag with 1000 ppmv inlet H_2S concentration at 500°C is much higher than the others.

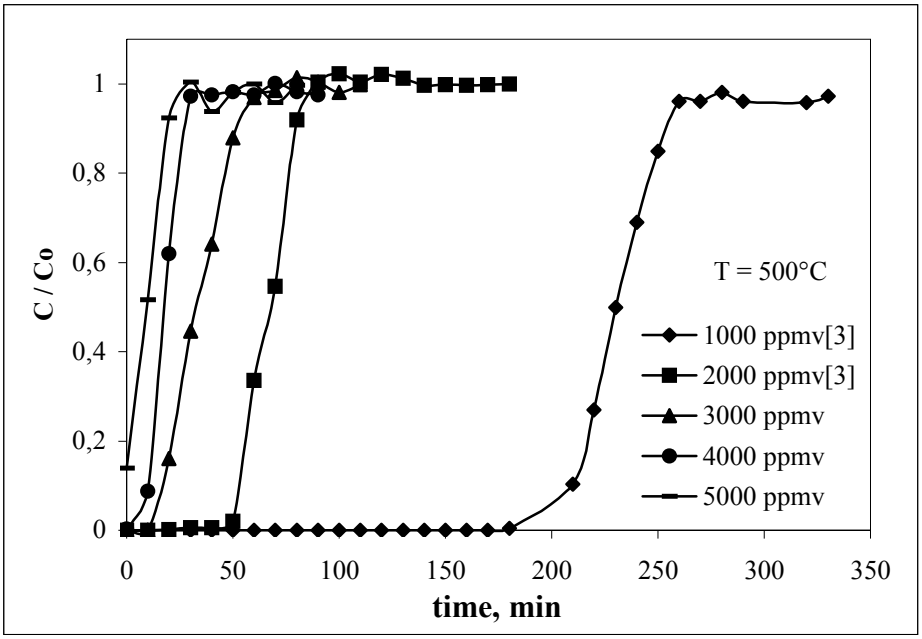

Figure 4.5 Breakthrough Curves for H_2S at 500°C (steel slag as sorbent)

Breakthrough curves for 1000, 2000, 3000, 4000 and 5000 ppmv inlet H_2S concentrations at the reaction temperature of 600°C are given in Figure 4.6 in order to compare the effect of inlet concentrations at the same reaction temperature. The result is the same as in the previous case. The sorption capacity of the sorbent decreases with increasing inlet H_2S concentration. The sorption capacity of the sorbent for 1000 ppmv inlet H_2S concentration at 600°C is quite high.

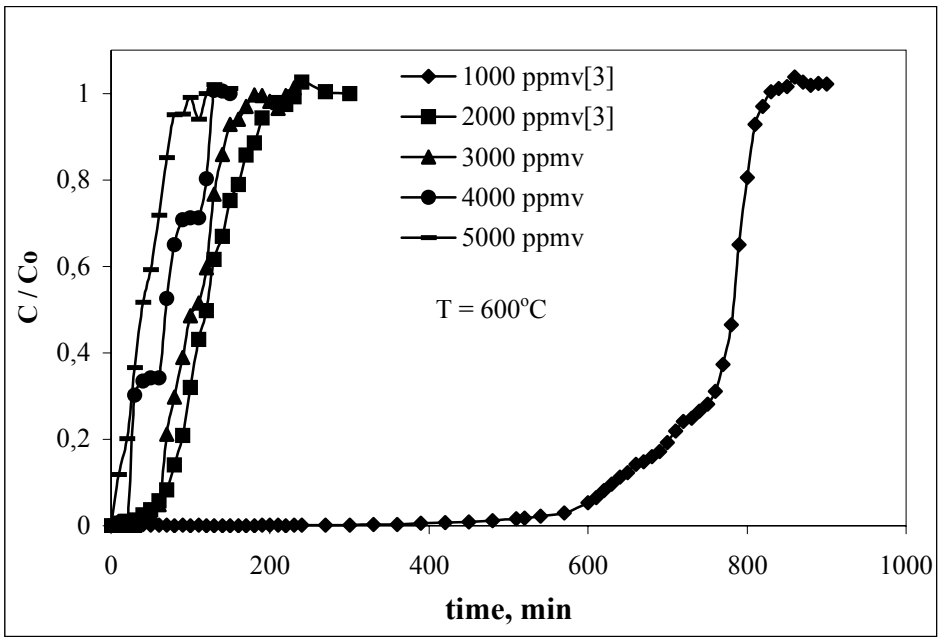

Figure 4.6 Breakthrough Curves for H_2S at 600°C (steel slag as sorbent)

The H_2S sorption capacities of steel slag at different temperatures and for different inlet H_2S concentration are given in Table 4.1. The data for 1000 and 2000 ppmv inlet H_2S concentartions are taken from Sarıçiçek [3]. From this table, it is seen that the sorption capacity of the sorbent decreases with increasing inlet H_2S concentration when the reaction temperature is kept constant except for the case of 4000 ppmv-inlet H_2S concentration at the temperature of 700°C. There is a very slight increase in sorption capacity although it is expected to decrease. This difference is very small and can be attributed to an experimental error. Also, the sorption capacities of the sorbent increases when the reaction temperature increases with the same inlet H_2S concentration. As can be seen from the table, the H_2S sorption capacity of this sorbent is the highest at 600°C (2.20 g S / 100 g sorbent) with an inlet H_2S concentration of 1000 ppmv.

It is expected that the reaction rate will increase with the increase of temperature. As a result, higher amount of H_2S will react with the sorbent and therefore, sulfur capacity of the sorbent (g S / 100 g sorbent) will increase with increase in temperature. However, as the inlet H_2S concentration increases, the sorption capacity decreases. This can be due to a formation of a dense product layer on the surface of the sorbent particles and this layer does not let the gas molecules further into the sorbent particles.

Table 4.1 Sorption Capacities of Steel Slag

Sulfidation Temperatures	Sulfur capacity, g S / 100 g Sorbent				
	Inlet H_2S Concentrations, ppmv				
	1000*	2000*	3000	4000	5000
400°C	0.80	0.17	-	-	-
500°C	0.88	0.51	0.18	0.12	0.09
600°C	2.20	0.93	0.58	0.51	0.40
700°C	-	-	0.92	0.95	0.72

*These data were obtained from Sarıçiçek [3]

4.1.2 Sulfidation Experiments with Zinc Slag

The same zinc slag samples were used in this study as in the previous study [3]. Sulfidation experiments were carried out with 3000, 4000 and 5000 ppmv inlet H_2S concentrations at reaction temperatures of 500°C and 600°C for zinc slag. Zinc slag having 2-3 mm particle size was used in these experiments as in the previous study [3].

The reaction temperature of 700ºC was not tried in these experiments because ZnO can be reduced to Zn in the reducing atmosphere and can evaporate as Zn vapor at these temperatures because melting point of zinc is 750ºC.

Breakthrough curves were plotted in order to observe the effect of reaction temperature on the sorption capacity of the sorbent. Breakthrough curves obtained for 3000 ppmv inlet H_2S concentration at temperatures of 500°C and 600°C are given in Figure 4.7. As can be seen from the figure, the capacity of the sorbent increases with increasing temperature. That is, the sorbent can desulfurize the gas more effectively at higher temperatures as compared to lower reaction temperatures, because the reaction rate is faster at higher temperatures. The 200-ppmv breakthrough concentration is reached in about 45 min and 115 min at the reaction temperatures of 500°C and 600°C, respectively. Time interval with zero H_2S concentration in the outlet stream is 30 min at 500°C, and 100 min at 600°C. This efficiency is quite good as compared to the steel slag at the same conditions, about 5 times as much. This is a very promising result.

Figure 4.8 shows the breakthrough curves obtained for 4000 ppmv inlet H_2S concentration at 500°C and 600°C. Again, the sorption capacity of the sorbent increases with increasing temperature due to increase in reaction rate with temperature. 200-ppmv breakthrough concentration of H_2S is achieved in about 40 min and 70 min at 500°C and 600°C, respectively. At 500°C, no H_2S concentration in the outlet stream is observed for a period of 40 min from the start of the reaction. This period is 50 min at 600°C. These are very encouraging results because there are few sorbents in the literature which can keep the outlet H_2S concentration at 1-2 ppmv for this long. However, the sorbent used here is a waste and almost free of charge. The other sorbents are manufactured.

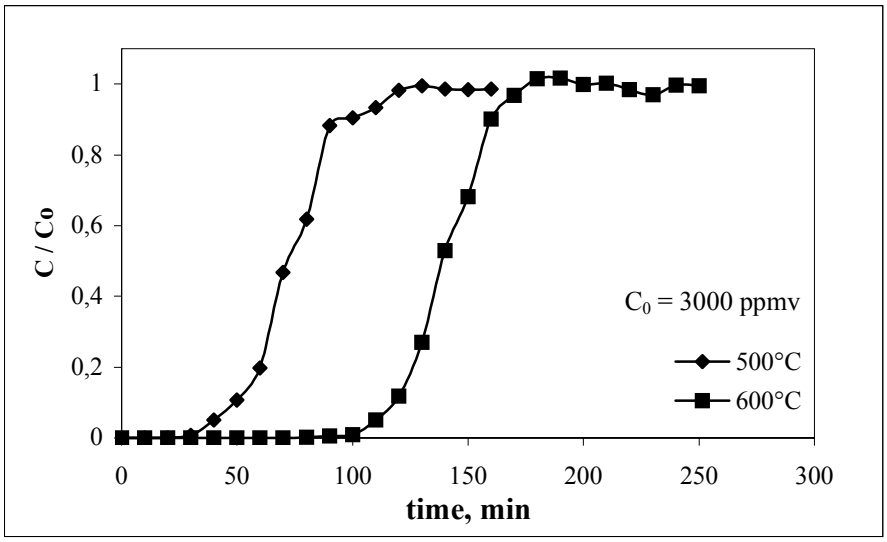

Figure 4.7 Breakthrough Curves for H_2S at Different Temperatures with 3000 ppmv Inlet Concentration (zinc slag as sorbent)

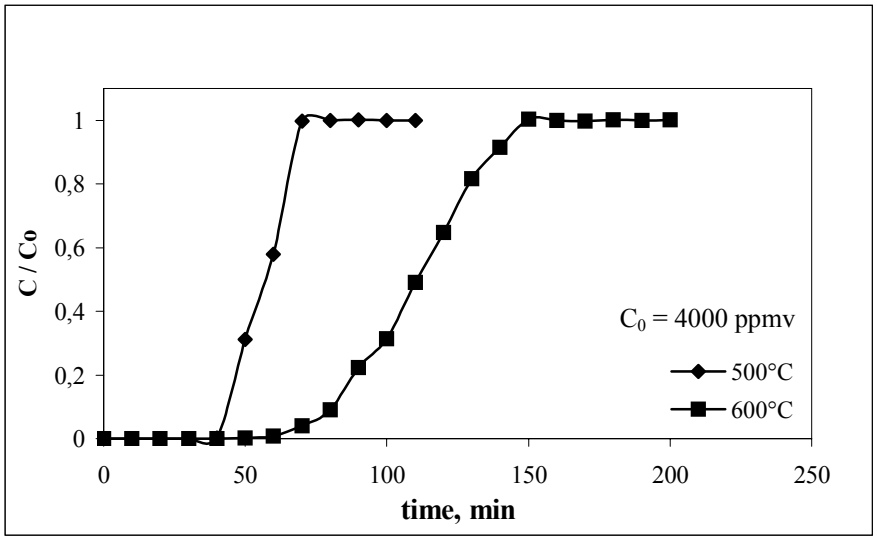

Figure 4.8 Breakthrough Curves for H_2S at Different Temperatures with 4000 ppmv Inlet Concentration (zinc slag as sorbent)

The breakthrough curves obtained for 5000 ppmv-inlet H_2S concentration at 500°C and 600°C are given in Figure 4.9. It is again seen that, the sorbent capacity is higher at 600°C than at 500°C. 200-ppmv breakthrough concentration is obtained in about 15 min and 30 min at 500°C and 600°C, respectively. The time interval with no H_2S concentration at the exit of the reactor is about 10 min and 30 min at 500°C and 600°C, respectively. The time interval with no exit H_2S concentration gets smaller as the inlet H_2S concentration increases.

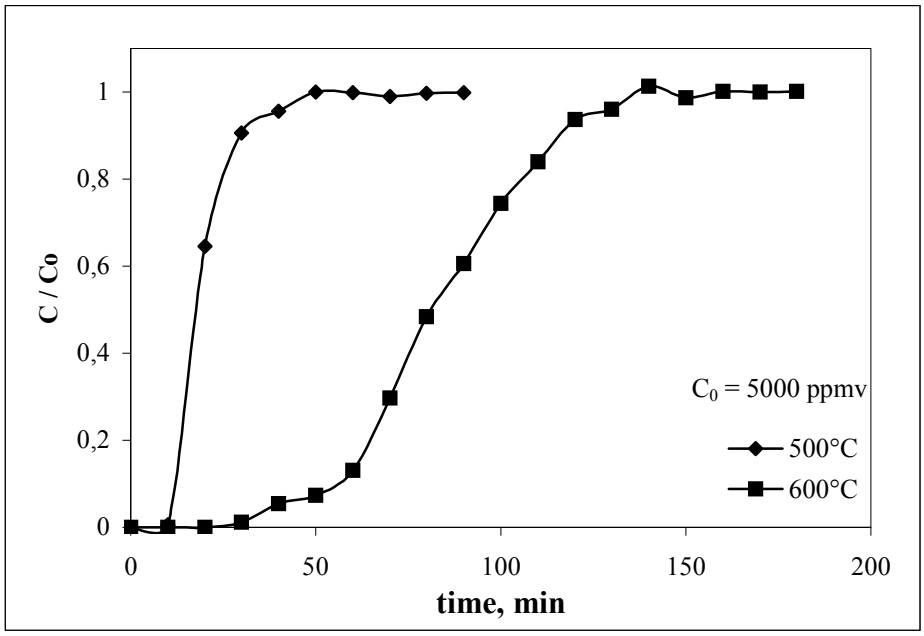

Figure 4.9 Breakthrough Curves for H_2S at Different Temperatures with 5000 ppmv Inlet Concentration (zinc slag as sorbent)

This phenomena can be explained by considering the reactions at the surface of the sorbent. With increase in the inlet concentration of H_2S, the particles are exposed to a higher concentration of H_2S in the gas phase. Although the

reaction takes place fast at the beginning of the reaction, it is thought that due to formation of ZnS, FeS_2, CaS and MnS, a dense product layer is formed on the surface of the sorbent particles and the diffusion of the H_2S molecules to the inside of the particles are hindered. Therefore, after some time, the inlet H_2S concentration starts to appear at the outlet gas. The breakthrough is reached much earlier than at low concentrations.

In Figure 4.10, breakthrough curves obtained for 3000, 4000 and 5000 ppmv H_2S inlet concentration at the reaction temperature of 600°C are given for the purpose of showing the effect of inlet concentration on the sorption capacity of the sorbent. The sorption capacity of the sorbent decreases with increasing inlet H_2S concentration. That is, increase in the inlet H_2S concentration affects the sorption capacity of the sorbent adversely.

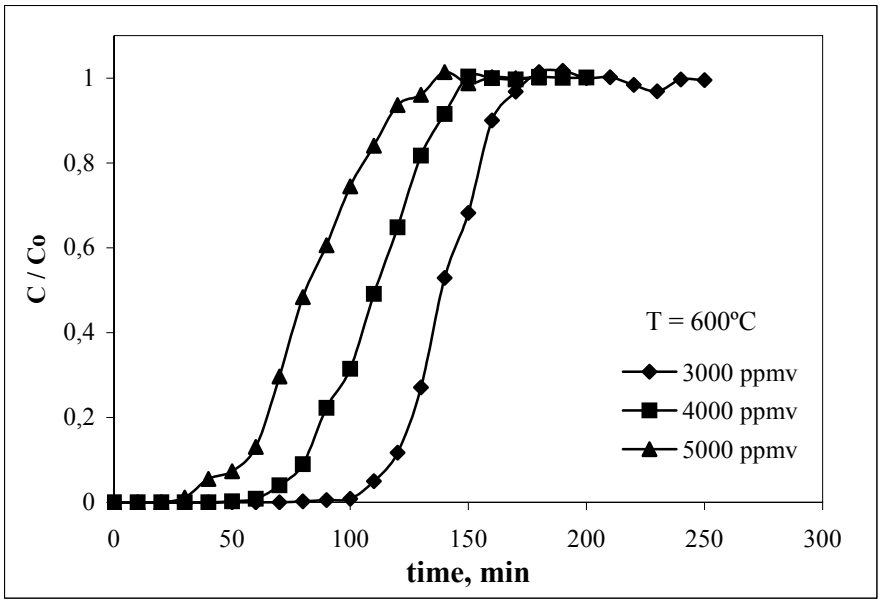

Figure 4.10 Breakthrough Curves for H_2S at 600°C Showing the Effect of Inlet Concentration (zinc slag as sorbent)

In order to see the effect of inlet H_2S concentration on the sorbent capacity in a better perspective, the data of inlet H_2S concentrations of 1000 ppmv and 2000 ppmv at the temperatures 500°C and 600°C were taken from Sarıçiçek [3]. These data were combined with the data obtained in this study and plotted in Figure 4.11.

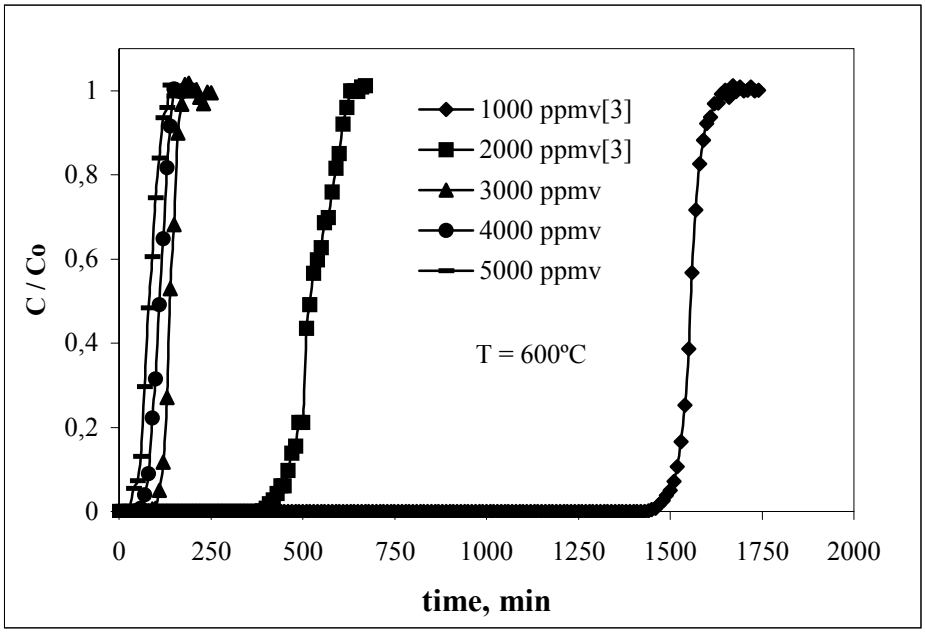

Figure 4.11 Breakthrough Curves for H_2S at 600°C (zinc slag as sorbent)

Figure 4.11 illustrates the breakthrough curves obtained for 1000, 2000, 3000, 4000 and 5000 ppmv inlet H_2S concentrations at 600°C. The sorption capacity decreases significantly with increasing inlet H_2S concentration. The sorption capacity of zinc slag with 1000-ppmv inlet H_2S concentration at 600°C is about 5 times higher than the sorption capacity of sorbent with 5000-ppmv inlet H_2S concentration at the same temperature. This is a very good result for removing H_2S in a hot gas cleanup system at lower concentrations. The time on line with

no H_2S concentration is about 1500 min (25 hours) at 1000 ppmv inlet H_2S concentration and about 500 min (8.3 hours) at 2000 ppmv inlet H_2S concentration.

As can be seen from Figure 4.11, the breakthrough curves for 3000, 4000 and 5000 ppmv inlet H_2S concentrations are very close to each other. This means that their breakthrough times are also close to each other, about 100-125 min. This figure shows very clearly that, there is a hinderence of H_2S sorption at these concentrations and this could be all due to the formation of dense product layer on the surface of the sorbent particles at high concentrations.

The H_2S sorption capacities of zinc slag at different temperatures and for different inlet H_2S concentration are given in Table 4.2. From this table, it is seen that the sorption capacity of the sorbent decreases with increasing inlet H_2S concentration and the sorption capacities of the sorbent increases with increasing reaction temperature.

Table 4.2 Sorption Capacities of Zinc Slag

Sulfidation Temperatures	Sulfur capacity, g S / 100 g Sorbent				
	Inlet H_2S Concentrations, ppmv				
	1000*	2000*	3000	4000	5000
400°C	1.17	0.78	-	-	-
500°C	2.78	1.87	0.39	0.33	0.18
600 °C	5.78	3.88	0.75	0.79	0.75

*These data were obtained from Sarıçiçek [3]

4.2 Cyclic Tests

Cyclic tests were performed in order to determine the regenerability of the sorbents used in this study. 3 ½ successive cycles were applied to both steel slag and zinc slag at 500°C. One cycle consisted of one sulfidation and one regeneration experiment.

In sulfidation experiments, the sorbent was exposed to H_2S and the exit H_2S concentration was measured by using GC having a PFP detector. Breakthrough curves obtained for inlet H_2S concentrations were plotted.

Regeneration experiments were carried out at the same conditions with the sulfidation experiments. During regeneration experiments, air was used in order to regenerate the sulfided sorbent. Sulfur in the metal sulfides in sulfided sorbent was replaced with oxygen in the air and result was the formation of metal oxide and SO_2. In regeneration experiments, SO_2 concentration from the reactor was measured in the GC and breakthrough curves for exit SO_2 concentration were plotted against reaction time.

4.2.1 Cyclic Tests of Steel Slag

The breakthrough curves obtained after four successive sulfidation and regeneration of steel slag sorbent are given in Figure 4.12. The sorption capacity of the steel slag decreases as the number of sulfidation increases. There is a slight difference between the first and the second sulfidation, although there is no considerable difference between the third and the fourth sulfidation.

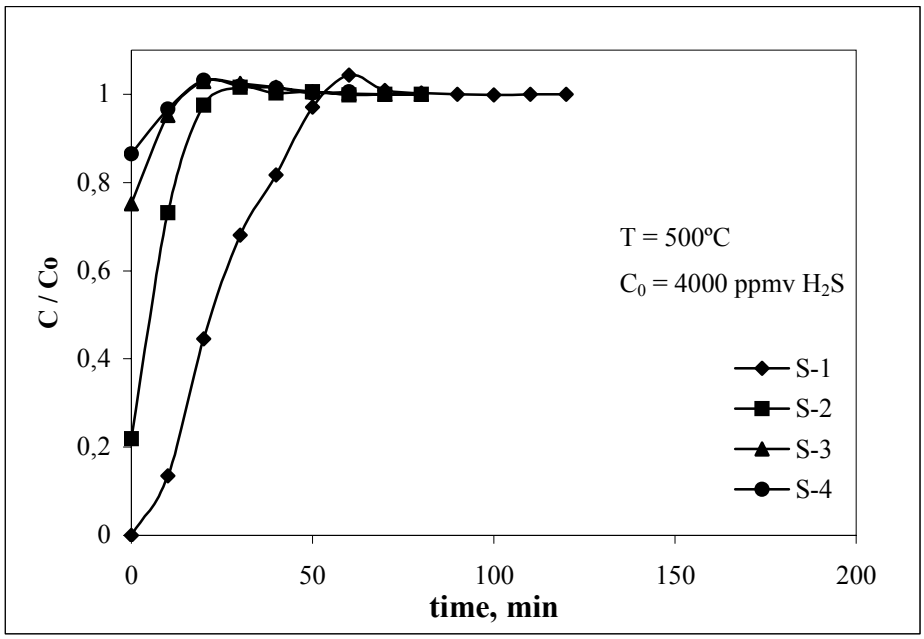

Figure 4.12 Breakthrough Curves for H_2S for Four Successive Sulfidation at 500°C with 4000 ppmv Inlet Concentration
(S = Sulfidation Experiment)

Figure 4.13 illustrates the exit SO_2 concentration during the regeneration experiments. At first, the concentration of exit SO_2 is about 800 ppmv during the beginning of the first regeneration. Then, the exit concentration decreases sharply in the first 10 min of the regeneration, then reaches to zero after 10 min, indicating the regeneration of the sorbent is over. Theoretically, the exit SO_2 concentration should be zero when the regeneration is over. However, the exit SO_2 concentration is about 1.5 ppmv after regeneration is completed. The reason for this may be the formation of metal sulfate instead of metal oxide in the presence of oxygen.

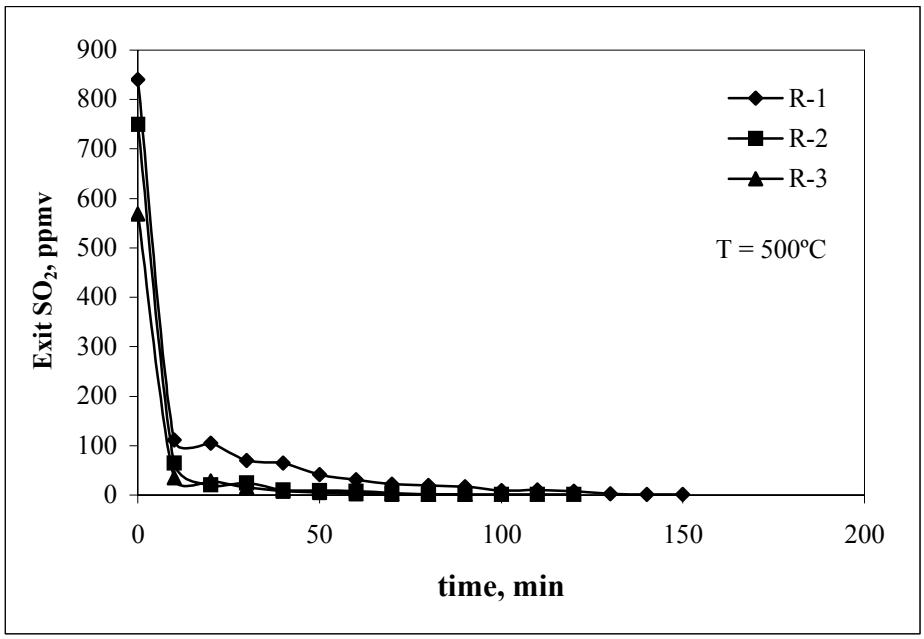

Figure 4.13 Breakthrough Curves for SO_2 During Regeneration at 500°C (R=Regeneration Experiments)

The sorption capacities of the steel slag after each sulfidation experiment are given in Table 4.3. As the sulfidation number increases, the sorption capacity of the steel slag decreases. Metal sulfate formations in the sulfided sorbent may prevent the complete regeneration and this may affect the sorption capacity of the sorbent adversely.

4.2.2 Cyclic Tests of Zinc Slag

The breakthrough curves for four successive sulfidation of zinc slag at 500°C are given in Figure 4.14. Sorption capacity of the zinc slag decreases sharply especially after the first sulfidation.

Table 4.3 Sorbent Capacities of Steel Slag During Cyclic Test

(T = 500ºC, C_o=4000 ppmv H_2S)

Sulfidation number	Sorbent capacity, g S/100 g Sorbent
S-1	0.12
S-2	0.048
S-3	0.006
S-4	0.004

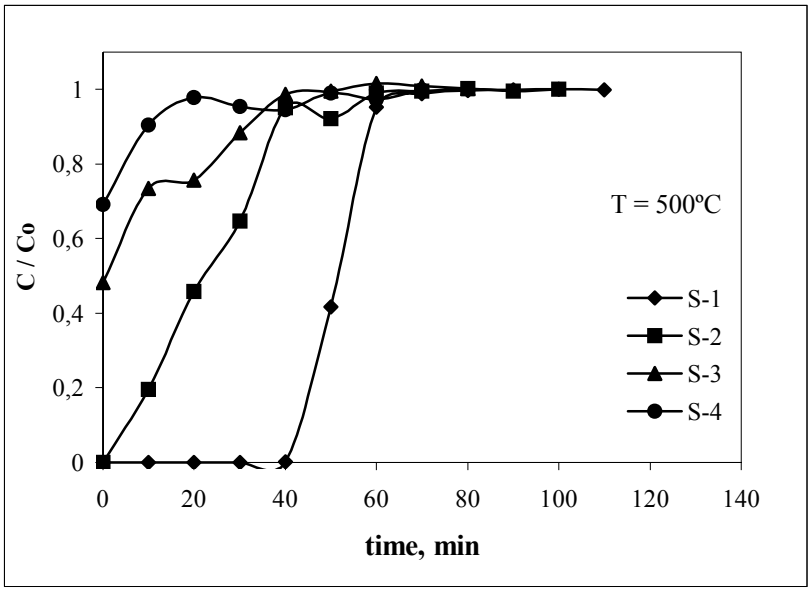

Figure 4.14 Breakthrough Curves for H_2S for Four Successive Sulfidation at 500°C with 5000 ppmv Inlet Concentration

(S = Sulfidation Experiment)

Figure 4.15 shows the SO_2 concentration evolved during the regeneration of the sulfided zinc slag. The amount of exit SO_2 is about 350 ppmv firstly, however it decreases to zero as the regeneration of the sulfided zinc slag is completed. Exit SO_2 concentration should reduce to zero at the end, however it reduced at the end to about 6 ppmv in this study as in the case of steel slag.

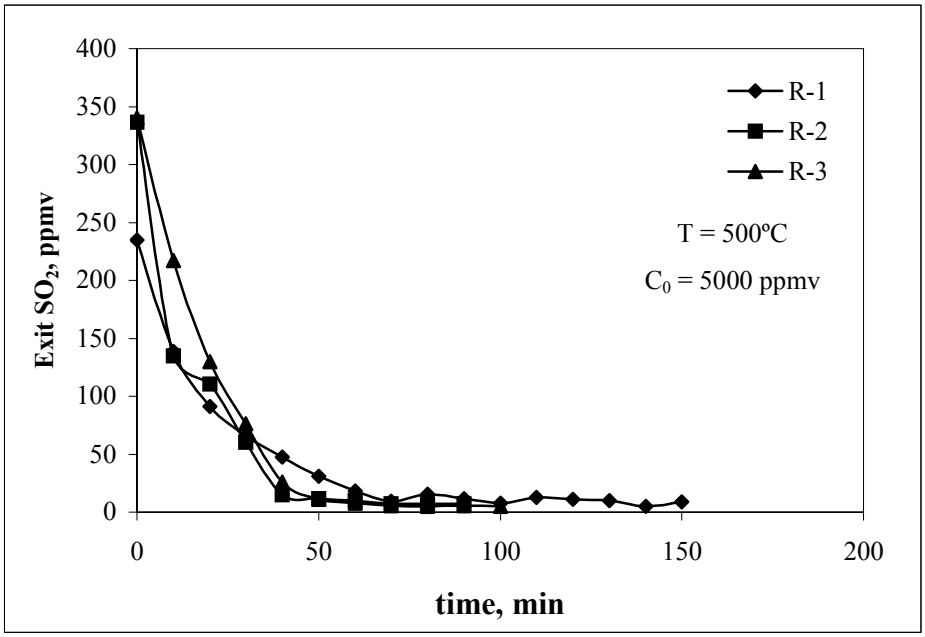

Figure 4.15 Breakthrough Curves for SO_2 During Regeneration at 500°C (R = Regeneration Experiments)

Sorption capacities of the zinc slag after each sulfidation run are given in Table 4.4. Again, the sorption capacity of the zinc slag decreases with increasing sulfidation number. This may be due to the formation of the metal sulfate rather than metal oxide in the presence of oxygen. However, this is not very important because the cost of the both steel and zinc slag is very low, almost

free of charge. Both steel slag and zinc slag after several regeneration can be disposed in a landfill area because metal sulfate is a stable compound and it does not cause environmental pollution. However, the metal sulfate concentrations of the used sorbents should be checked before disposal.

Table 4.4 Sorbent Capacities of Zinc Slag During Cyclic Test

(T = 500ºC, C_o=5000 ppmv H_2S)

Sulfidation number	Sorbent capacity, g S/100 g Sorbent
S-1	0.210
S-2	0.211
S-3	0.079
S-4	0.036

4.3 Physical Characterization After Sulfidation

4.3.1 Steel Slag

SEM photographs of the steel slag after sulfidation experiments at different temperatures are given in Figure 4.16. There are morphological changes in the structure of the steel slag. In fresh (unused) steel slag, rod shape and crystalline structures were commonly seen in Figure 3.3. However, after sulfidation of the steel slag, these rod shape structures are not seen, but crystalline structures are there. As it was explained before, when the inlet concentration of H_2S increases, there is a hindrance of H_2S sorption due to the formation of dense product layer on the surface of the sorbent particles. Very interestingly, in

Figure 4.16c, the SEM photograph shows very clearly the formation of the dense product layer and the decrease of the porosity of the particles at 4000 ppmv inlet H_2S concentration. The surface is densely packed and looks very different than the previous photographs although the magnification is the same with the previous photographs.

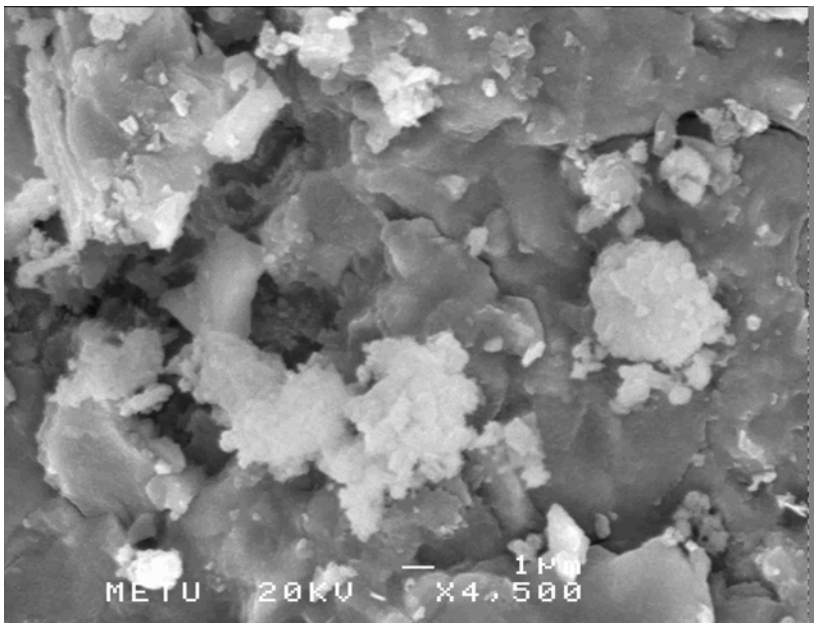

Figure 4.16a SEM Photographs of Steel Slag After Sulfidation with Inlet Concentration of 4000 ppmv H_2S
500°C (x4500)

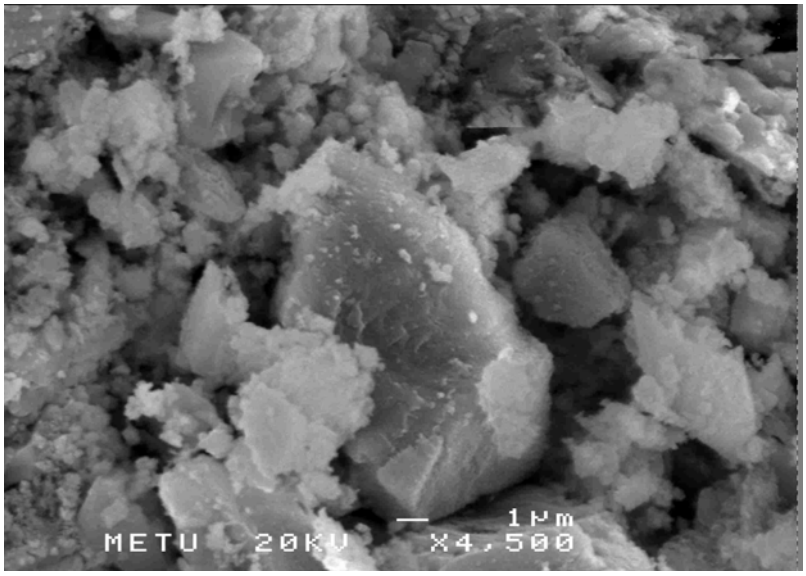

Figure 4.16b SEM Photographs of Steel Slag After Sulfidation with Inlet Concentration of 4000 ppmv H_2S
600°C (x4500)

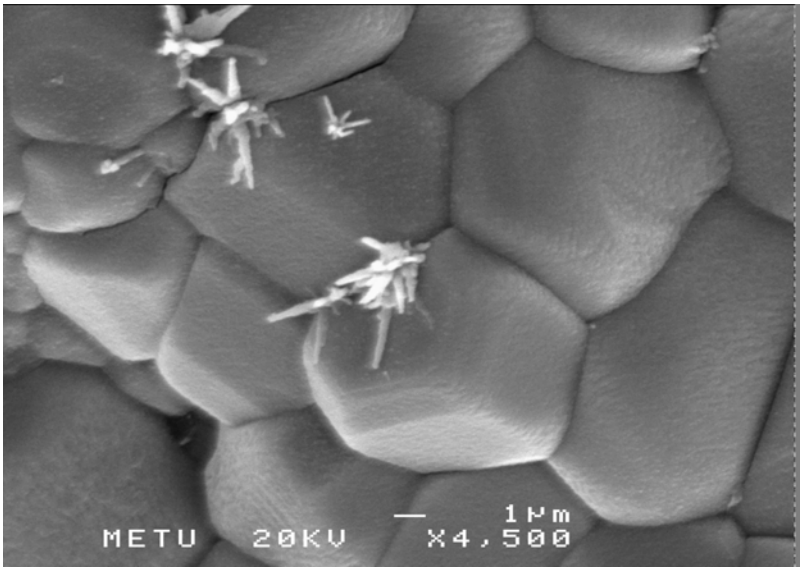

Figure 4.16c SEM Photographs of Steel Slag After Sulfidation with Inlet Concentration of 4000 ppmv H_2S
700°C (x4500)

4.3.2 Zinc Slag

SEM photographs of the zinc slag after sulfidation experiments at different temperatures are given in Figure 4.17. From this figure, some morphological changes in the structure of the zinc slag can be observed. Fresh zinc slag possessed a very porous structure. However, after sulfidation of the zinc slag, the crystalline structure has changed to smoother structure.

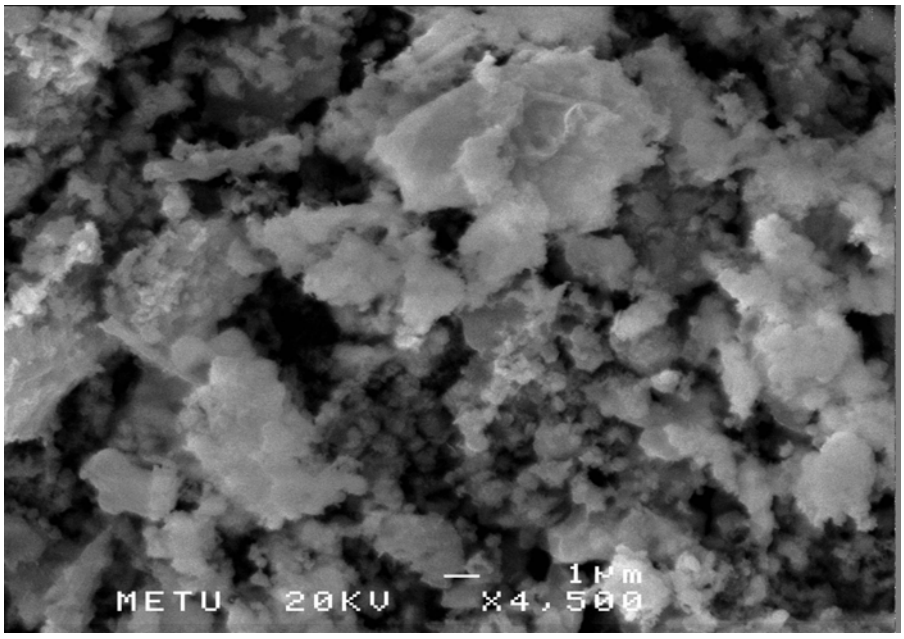

Figure 4.17a SEM Photographs of Zinc Slag After Sulfidation with Inlet Concentration of 5000 ppmv H_2S
500°C (x4500)

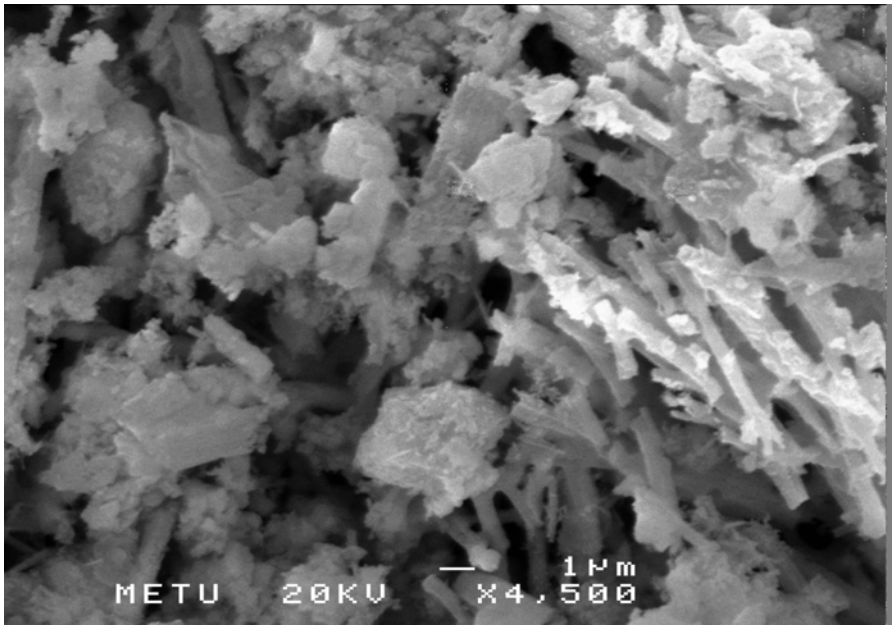

Figure 4.17b SEM Photographs of Zinc Slag After Sulfidation with Inlet Concentration of 5000 ppmv H_2S
600°C (x4500)

4.4 Chemical Characterization After Sulfidation

XRD analysis was carried out in order to determine the formation of possible chemical phases in the sorbent after sulfidation experiments. XRD analysis for the steel slag after sulfidation could be done only. Figure 4.18 shows the result of XRD analysis for steel slag which was exposed to 4000 ppmv inlet H_2S concentration at 700ºC. As can be seen from figure, FeS and CaS formed during sulfidation. Also, $CaFeSiO_4$, which was present in the fresh (unused) steel slag, is still observed after sulfidation.

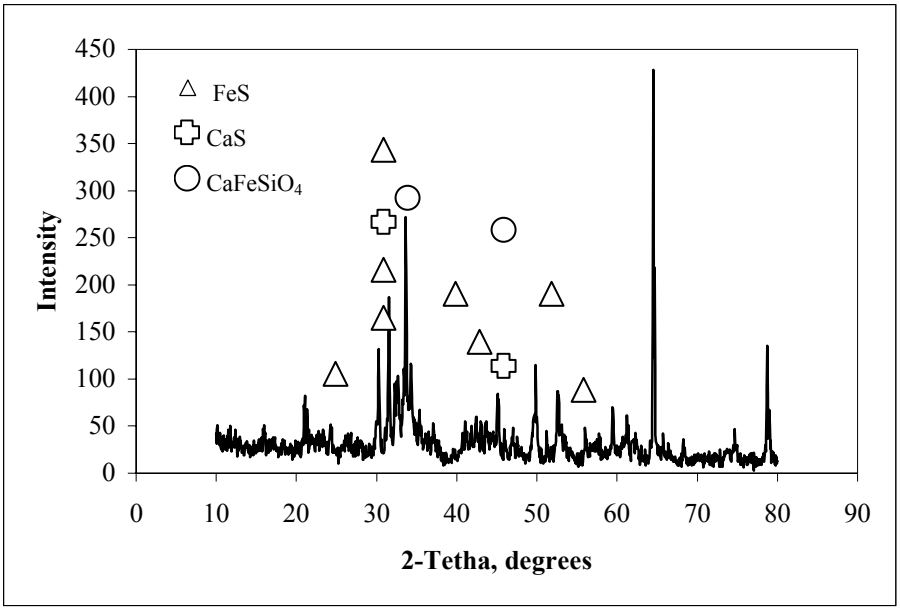

Figure 4.18 XRD Graph of Steel Slag After Sulfidation at 700°C with 4000 ppmv H_2S

4.5 Deactivation Model Predictions

Deactivation model was applied in this study. The breakthrough equation Eq. (4.1) derived by Yasyerli et al. [26] was used for prediction of the breakthrough curves.

$$\frac{C_A}{C_{A0}} = \exp\left\{\frac{\left[1-\exp\left(\frac{k_0 W}{Q}\left(1-\exp(-k_d t)\right)\right)\right]}{\left[1-\exp(-k_d t)\right]}\exp(-k_d t)\right\} \qquad (4.1)$$

where C_A = concentration of reactant gas, kmol/m^3

W = sorbent mass, kg

Q = volumetric flowrate of gas, m^3/min

k_0 = initial sorption rate constant, m^3/kg.min

k_d = deactivation rate constant, $(min^{-1})\times 10^2$

Arrhenius equation was used for the determination of the initial sorption rate constant k_0 at different temperatures.

$$k_0 = A \times \exp\left(-E_a / RT\right) \tag{4.2}$$

where k_0 is the initial sorption rate constant [cm^3/min.g], A is a pre-exponential constant [cm^3/min.g], E_a is the activation energy [kJ/mole], R is the gas constant [8.314 J/mole.K], and T is the temperature [K].The activation energy was taken from the literature for similar H_2S sorption reactions as 6.55 kJ/mole [40]. k_0 values for different temperatures were calculated according to Eq. (4.2). After determining the estimated k_0 values, k_d and C_A/C_{A0} values were found by fitting the breakthrough curves obtained experimentally. Analysis of the experimental breakthrough data obtained for both steel slag and zinc slag in the temperature range between 500°C and 700°C gave very good agreement with Eq. (4.1).

4.5.1 Regression Analysis for Steel Slag

The results of the regression analysis of the data obtained for steel slag are given in Table 4.5. From Table 4.5, it is seen that the initial reaction rate constant k_0 fluctuates little at the same temperatures. The initial rate constant k_0 increases with increasing temperature showing that the gas-solid reaction is more active at higher temperatures. Furthermore, the deactivation rate constant k_d increases with increasing inlet H_2S concentration because high inlet H_2S concentration increases the formation of dense product layer over the sorbent. The higher the H_2S concentration, the larger becomes the k_d. This is an indication and proof of the formation of a dense product layer over the sorbent.

Table 4.5 Rate Parameters for Steel Slag

Inlet H_2S Concentration	Temperature , ºC					
	500		600		700	
	k_0 $cm^3/g.min$	k_d $(min^{-1})\times10^2$	k_0 $cm^3/g.min$	k_d $(min^{-1})\times10^2$	k_0 $cm^3/g.min$	k_d $(min^{-1})\times10^2$
3000 ppmv	158.04	0.311	205.69	0.331	225.37	0.111
4000 ppmv	152.36	0.596	198.86	0.602	218.19	0.146
5000 ppmv	150.46	0.645	196.56	0.200	218.19	0.265

Figures 4.19 and 4.20 show the breakthrough curves obtained by experimental data and deactivation model prediction using the Eq. (4.1) with different inlet H_2S concentrations at different temperature for steel slag. From these figures, it can be concluded that the predicted breakthrough curves fit the experimental curves quite well.

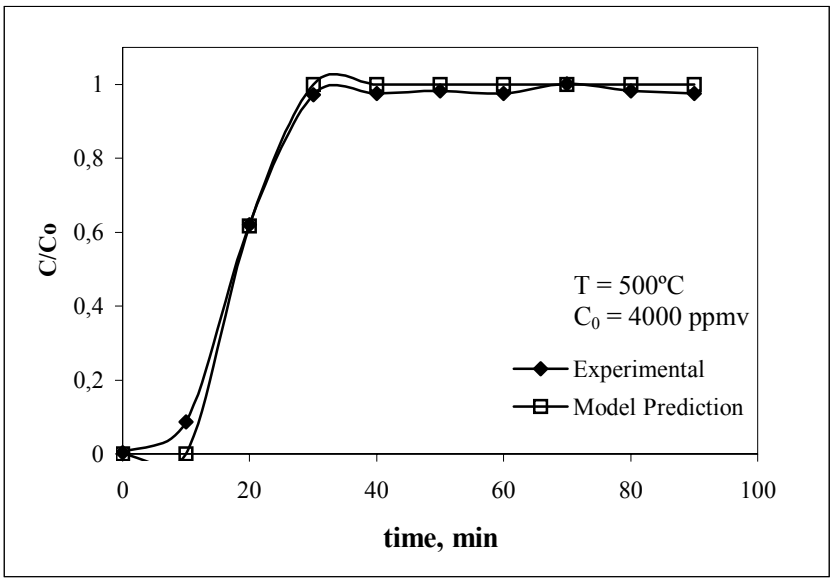

Figure 4.19 Comparison of Breakthrough Curves for 4000 ppmv H_2S at 500°C Obtained by Deactivation Model Prediction and Experimental Data

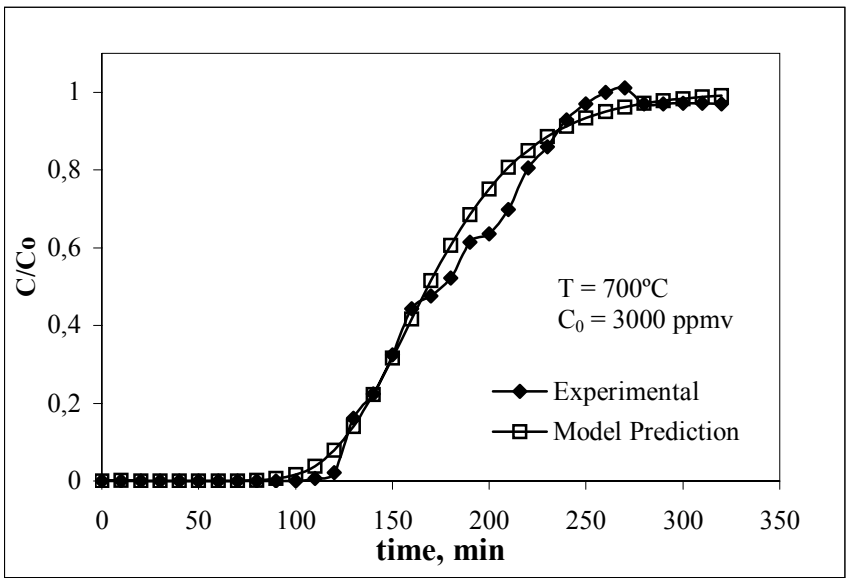

Figure 4.20 Comparison of Breakthrough Curves for 3000 ppmv H_2S at 700°C Obtained by Deactivation Model Prediction and Experimental Data

Activation energies of steel slag at different temperature were calculated by using the k_0 values in Table 4.5 according to Eq. (4.2). The results are given in Table 4.6. The activation energy decreases with increasing temperature according to the Arrhenius equation (Eq. (4.2)).

Table 4.6 Activation Energies of Steel Slag

Temperature, °C	Activation Energy, kJ/mole
500	7.46
600	6.50
700	6.46

4.5.2 Regression Analysis for Zinc Slag

Table 4.7 illustrates the results of the regression analysis of the data obtained for zinc slag. The initial reaction rate constant k_0 is almost the same for the concentrations investigated independent of the inlet H_2S concentration and it increases with increasing temperature. Also, the deactivation rate constant k_d increases with increasing inlet H_2S concentration. This result also shows the formation of a dense product layer over the sorbent and as the inlet H_2S concentration gets higher, the resistance offered by this layer to sorption of H_2S becomes larger.

Table 4.7 Rate Parameters for Zinc Slag

Inlet H_2S Concentration	Temperature , ºC			
	500		600	
	k_0 $cm^3/min.g$	k_d $(min^{-1})\times10^2$	k_0 $cm^3/min.g$	k_d $(min^{-1})\times10^2$
3000 ppmv	95.37	0.102	196.56	0.109
4000 ppmv	95.37	0.131	198.86	0.156
5000 ppmv	94.13	0.366	197.25	0.231

Activation energies of zinc slag at different temperature were calculated using the k_0 values in Table 4.7 according to Eq. (4.2). The results are given in Table 4.8. As expected, the deactivation energy is higher at 500ºC than at 600ºC, according to the Arrhenius equation.

Table 4.8 Activation Energies of Zinc Slag

Temperature, °C	Activation Energy, kJ/mole
500	10.55
600	6.60

Comparison of the predicted breakthrough curves and breakthrough curves obtained for zinc slag by experimental data for different inlet H_2S concentration at different temperatures are given in Figures 4.21 and 4.22. The experimental breakthrough curve gives a very good agreement with the breakthrough equation derived.

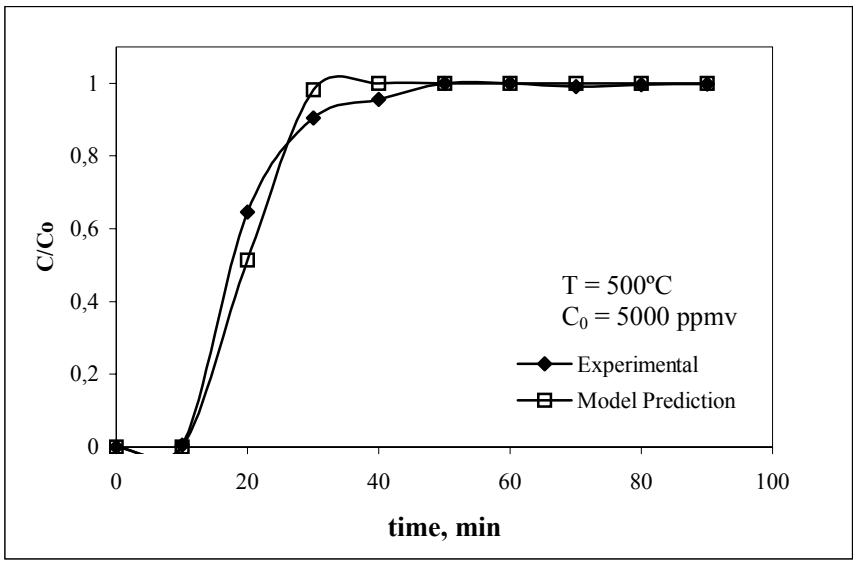

Figure 4.21 Comparison of Breakthrough Curves for 5000 ppmv H_2S at 500°C Obtained by Deactivation Model Prediction and Experimental Data

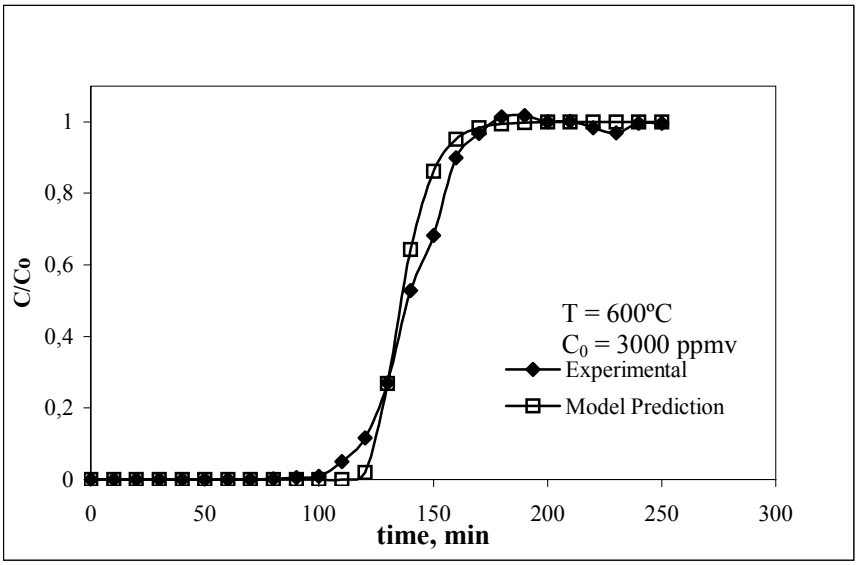

Figure 4.22 Comparison of Breakthrough Curves for 3000 ppmv H_2S at 600°C Obtained by Deactivation Model Prediction and Experimental Data

4.6 Comparison of Results with the Data from Literature

In the literature, there are many studies for desulfurization of hot coal gas with different metal oxide sorbents. The comparison of these studies with the recent study with respect to the sorption capacities of the sorbents and experimental conditions are given in Table 4.9.

As can be seen from Table 4.9, the highest sorption capacity, 23 g S / 100 g sorbent, belongs to the half calcinated dolomite ($CaCO_3$.MgO). The sorption capacity of zinc ferrites is also quite high with respect to the other sorbents. However, the use of these sorbents may increase the cost of hot gas cleanup system because these sorbents need to be manufactured with special processes. Although the sorption capacities of steel and zinc slags are lower as compared to zinc ferrites or copper based sorbents, the use of these waste materials would be more suitable from the economical point of view, because they are almost free of charge.

In addition to this economical advantage, there is another positive point for the waste materials which is the structural stability. Zinc ferrite, for example, decrepitates after some sulfidation and regeneration reactions and the sorbent particles dissociates. On the other hand, the steel slag and zinc slag has gone through sinterization reactions and silicates are formed. Therefore, these formations make the waste material structually stable. This is a very big advantage for these sorbents. Therefore, steel slag from iron and steel production plant and zinc slag from zinc production plant are two suitable candidates for hot gas desulfurization. They are abundant and they are almost free of charge. The sorption capacity of zinc slag is higher than that of steel slag. The mixture of steel and zinc slags at different ratios also gives good results as shown by Sarıçiçek [3].

Table 4.9 Comparison of Sorption Capacities of Different Sorbents

Sorbent Type	Reference	Temperature, °C	H_2S concentration, ppmv	Sorbent Capacity, g S/ 100 g Sorbent
Steel Slag	Sarıçiçek [3]	400 – 600	1000 – 2000	0.17 – 2.20
Steel Slag	This Study	500 – 700	3000 – 5000	0.09 – 0.95
Zinc Slag	Sarıçiçek [3]	400 – 600	1000 – 2000	0.78 – 5.78
Zinc Slag	This Study	500 – 600	3000 – 5000	0.18 – 0.79
25% Zn Slag+75% Fe Slag	Sarıçiçek [3]	500	2000	0.75
50% Zn Slag+50% Fe Slag	Sarıçiçek [3]	500	2000	1.27
75% Zn Slag+25% Fe Slag	Sarıçiçek [3]	500	2000	2.55
Iron oxide waste (64% Fe)	Slimane and Abbasian [4]	500	20000	22.0
Zinc oxide waste (65% Zn)	Slimane and Abbasian [4]	500	20000	15.0
Zinc oxide waste (38% Zn)	Slimane and Abbasian [4]	500	20000	18.0

Table 4.9 Comparison of Sorption Capacities of Different Sorbents (Cont'd)

Zinc Ferrites	Jain et al. [41]	530 – 800	4500	16.0
Zinc Titanate Zn/Ti=1.5	Mojtahedi and Abbasian [42]	550 – 650	1500	4.0 – 5.0
Zinc Titanates + Molybdenum Oxide	Ayala and Jain [43]	540	10000	3.0
$CuO+Mn_2O_3$ on Alumina (49% and 17%)	Slimane and Abbasian [44]	450	20000	9.03
$CaCO_3.MgO$ half-calcinated Lhoist dolomite	Heesink [45]	750 – 850	15000	23.0

CHAPTER 5

CONCLUSIONS

It was proved that the steel and zinc slag have good desulfurization capacity for H_2S concentrations of 1000 ppmv and 2000 ppmv at the temperature range of 400°C and 600°C in the previous study done by Sarıçiçek in 2002. In this study, desulfurization capacities of the steel and zinc slag with higher H_2S concentrations, 3000 ppmv, 4000 ppmv and 5000 ppmv were determined because exit H_2S concentration from a typical gasifier is around 5000 ppmv.

The results of the sulfidation experiments have shown that the sorption capacity of both slags decreases with the increasing H_2S concentration. Moreover, the sorption capacities of the steel slag and zinc slag increase as the reaction temperature increases.

The highest desulfurization efficiency was obtained at 700°C with 3000 ppmv H_2S concentration for steel slag. The 200-ppmv breakthrough concentration was achieved in 100 min. Because of the volatility of zinc, the sulfidation experiments with zinc slag were carried out at the temperatures of 500°C and 600°C. Therefore, the highest H_2S removal efficiency for zinc slag was

achieved with 3000 ppmv H_2S concentration at the temperature of 600°C. The 200-ppmv breakthrough concentration was achieved in 115 min. Although the sulfidation temperatures of zinc slag are lower than that of steel slag, the H_2S removal efficiencies of zinc slag are higher than these of steel slag.

The results of the cyclic tests have shown that the sorption capacity of both slags decreases with increasing number of cycles. The sorption capacity of the steel slag after the first sulfidation decreased very sharply as compared to the zinc slag. That means zinc slag is more regenerable than steel slag.

"Deactivation model" was applied to the breakthrough data obtained for both steel and zinc slags. The initial activation rate of the slags increased with increasing temperature making the gas-solid reaction more active at higher temperatures. Furthermore, the deactivation rate constant decreased with the increasing inlet H_2S concentration indicating that a dense product layer is formed over the sorbent as the inlet H_2S concentration increases and the layer offers higher resistance for the sorption of H_2S by the sorbent. The experimental breakthrough curves gave very good agreement with the breakthrough curves obtained by using deactivation model.

In this study, the zinc slag was shown to be more effective in H_2S removal from the simulated coal gas due to its higher sulfidation capacity and regenerability.

REFERENCES

[1] M.C. Woods, S.K. Gangwal, D.P. Harrison, K. Jothimurugesan, 1990. "Reaction between Hydrogen Sulfide and Zinc Oxide-Titanium Oxide Sorbents, I.Single Pellet Kinetic Studies", Industrial Engineering and Chemical Engineering Research. Vol.29, pp. 1160-1166.

[2] R.B. Slimane, J. Abbasian, 2000. "Regenerable Mixed Metal Oxide Sorbents for Coal Gas Desulfurization at Moderate Temperatures", Advances in Environmental Research.Vol.4, No.2, pp.147-162.

[3] V. Sarıçiçek, 2002. Utilization of Metal Oxide-Containing Waste Metarials from Iron-Steel and Zinc Industries for Sorption of Hydrogen Sulfide. Master's Thesis, Middle East Technical University, Ankara.

[4] R.B. Slimane, J. Abbasian, 2001. "Utilization of Metal Oxide-containing Waste Materials for Hot Coal Gas Desulfurization", Fuel Processing Technology. Vol. 70, pp. 97-113.

[5] Electric Power Research Institute, Coal Gasification Systems: A guide to Status, Applications, and Economics, AP-3109, Research Project 2207, June 1983, Synthetic Fuels Associates, Inc., California, 94041.

[6] S.B. Alpert, M.J. Gluckman, 1986. "Coal Gasification Systems for Power Generation", Annual Review of Energy. Vol.11, pp.315-355.

[7] A.E. Van Diepen, 1996. "Effect of Process Conditions on Thermodynamics of Gasification", Presented in NATO Advanced Study Institute on Desulfurization of Hot Coal Gas with Regenerable Metal Oxide Sorbents: New Developments, Kuşadası, İzmir.

[8] R.E. Ayala, 1996. "Assessment of Coal Gasification Processes – Relevance to Sorbent Development", Presented in NATO Advanced Study Institute on Desulfurization of Hot Coal Gas with Regenerable Metal Oxide Sorbents: New Developments, Kuşadası, İzmir.

[9] P.W. Sage, S.J. Mills, 1996. "Overview of Clean Coal Technologies and Current Status of the Air Blown Gasification Cycle", Presented in NATO Advanced Study Institute on Desulfurization of Hot Coal Gas with Regenerable Metal Oxide Sorbents: New Developments, Kuşadası, İzmir.

[10] B. Liang, R.Korbee, A.W. Gerritsen, C.M. van den Bleek, 1999. "Effect of Manganese Content on the Properties of High Temperature Regenerative H_2S Acceptor", Fuel. Vol..78, pp 319-325.

[11] R.E. Ayala, 1996. "Application of IGCC Technology to Power Generation", Presented in NATO Advanced Study Institute on Desulfurization of Hot Coal Gas with Regenerable Metal Oxide Sorbents: New Developments, Kuşadası, İzmir.

[12] J.C. Corman, 1986. "System Analysis of Simplified IGCC Plants". General Electric Company, DOE/ET/14928-2233, NTIS/DE87002508. Springfield, VA: National Technical Information Service.

[13] D.P. Harrison, 1995. "Control of Gaseous Contaminants in IGCC Processes, an Overview", in Proceedings of the Twelfth Annual International Pittsburgh Coal Conference, pp. 1047-1052.

[14] J. Konttinen, W. Mojtahedi, 1993. "Gasifier Gas Desulfurization at High Temperature and Pressure", Kemia-Kemi, Vol. 20, pp. 847-851.

[15] S. Furfari, 1992. "Gasification and IGCC within the European Communities", Erdol und Kohle-Erdgas. Vol.45, No.7/8, pp.291-294.

[16] A.G.L. Van der Ham, R.H. Vanderbosch, W. Prins, W.P.M. Van Swaaij, 1996. "Desulfurization Process of Fuel Gas and Stagewise Desulfurization", Presented in NATO Advanced Study Institute on Desulfurization of Hot Coal Gas with Regenerable Metal Oxide Sorbents: New Developments, Kuşadası, İzmir.

[17] Clean Coal Technology, The New Coal Era, DOE/FE-0217P, Nov. 1989, US Department of Energy, Washington, DC, 20585.

[18] H. Short, R. Skole, 1988. "Coal said to Compete with Natural Gas in Power Scheme", Chemical Engineering. Vol.15, February, pp.35-36.

[19] A. Aksoy, 1994. Development of a Novel Regenerable Sorbent for Hot Gas Desulfurization. Master's Thesis, Middle East Technical University, Ankara.

[20] A.T. Atımtay, L.D. Gasper-Galvin, J.A. Poston, 1995. "Novel Supported Sorbent for Hot Gas Desulfurization", Environmental Science and Technology. Vol.27, No.7, pp. 1295-1303.

[21] M. Garcia-Calzada, G. Marban, A.B. Fuertes, 2000. "Stability and Oxidative Stabilisation of Sulphided Calcereous Sorbents from Entrained Flow Gasifiers", Chemical Engineering Science, Vol.55, pp. 3697-3714.

[22] I. R. Fantom, P. Cahill, P.W. Sage, 1996. "Hot Gas Cleaning – An Overview", Presented in NATO Advanced Study Institute on Desulfurization of Hot Coal Gas with Regenerable Metal Oxide Sorbents: New Developments, Kuşadası, İzmir.

[23] H.C. Frey, E.S. Rubin, 1992. "Integration of Coal Utilization and Environmental Control in Integrated Gasification Combined Cycle Systems", Environmental Science and Technology. Vol.26, No.10, pp 1982-1990.

[24] M. Flytzani-Stephanopoulos, Z. Li, 1996. "Kinetics of Sulfidation Reactions Between H_2S and Bulk Oxide Sorbents", Presented in NATO Advanced Study Institute on Desulfurization of Hot Coal Gas with Regenerable Metal Oxide Sorbents: New Developments, Kuşadası, İzmir.

[25] P.R. Westmoreland, J.B. Gibson, D.P. Harrison, 1976. "Evaluation of Candidate Solids for High-Temperature Desulfurization of Low-Btu Gases", Environmental Science and Technology. Vol.10, pp. 659-661.

[26] S. Yasyerli, G. Doğu, I. Ar, T. Doğu, 2001. "Activities of Copper Oxide and Cu-V and Cu-Mo Mixed Oxides for H_2S Removal in the Presence and Absence of Hydrogen and Predictions of a Deactivation Model", Ind. Eng. Chem. Res. Vol. 40, pp. 5206-5214.

[27] S.S. Tamhankar, S. Garimella, C.Y. Wen, 1981. "Kinetic Studies on the Reactions Involved in the Hot Gas Desulfurization Using a Regenerable Iron Oxide Sorbent-I", Chemical Engineering Science. Vol.36, pp. 1181-1191.

[28] R.E. Ayala, A.S. Feitelberg, A.H. Furman, 1995. "Development of a High-Temperature Moving Bed Coal Gas Desulfurization System", in Proceedings of the Twelfth Annual International Pittsburg Coal Conference (edited by S.H. Chiang), University of Pittsburgh, p.1053.

[29] R.H. Venderbosch, W. Prins, A.G.J. Van der Ham, 1996. "Removal of H_2S from Coal Gas: Effect of Various Parameters on the Desulfurization Efficiency", Presented in NATO Advanced Study Institute on Desulfurization of Hot Coal Gas with Regenerable Metal Oxide Sorbents: New Developments, Kuşadası, İzmir.

[30] F. Shultz, J.S. Berber, 1970. "Hydrogen Sulfide Removal from Hot Producer Gas with Sintered Absorbents", J.Air Pollution Control Association. Vol.20 p.2, February

[31] G.D. Focht, P.V. Ranade, D.P. Harrison, 1988. "High-Temperature Desulfurization Using Zinc Ferrite: Reduction and Sulfidation Kinetics", Chemical Engineering Science. Vol.43, No.11, pp. 3005-3013.

[32] J.K. Wright, A.L. Morrison, 1982. "Changes in Diffusivity Due to Sintering in Metallized Iron Oxide Pellets", Metallurgical Transactions-B. Vol.136, pp.518-520.

[33] T. Grindley, G. Steinfeld, 1983. "Zinc Ferrite as Hydrogen Sulfide Absorbent", Third Annual Contractors' Meeting on Contaminant Control in Hot Coal-Derived Gas Streams, Report No.DOE/METC/84-6.

[34] T. Grindley, G. Steinfeld, 1981. "Development and Testing of Regenerable Hot Coal Gas Desulfurization on Sorbents", Final Report, DOE/MC/16545-1125.

[35] S. Lew, A. F. Sarofirm, M. Flytzani-Stephanopoulos, 1992. "Sulfidation of Zinc Titanate and Zinc Oxide Solids", Ind. Eng. Chem. Res. Vol.31, pp.1890-1899.

[36] J.G. Peacey, W.G. Davenport, 1979. "The Iron Blast Furnace: Theory and Practice", Oxford; New York; Pergamon Press.

[37] M. C. Ocaktan, 1996. Recovery of Lead and Cadmium from ÇİNKUR Waelz Oxide by Using Chloridizing Volatilization Method. Master's Thesis, Middle East Technical University, Ankara.

[38] Y. Suyadal, M. Erol, H. Oğuz, 2000. "Deactivation Model for the Adsorption of Trichloroethylene Vapor on an Activated Carbon Bed", Ind. Eng. Chem. Res. Vol.39 p.724.

[39] T. Doğu, 1986. "Extension of Moment Analysis to Nonlinear Systems", AIChE J. Vol.32, p. 849.

[40] S. Yasyerli, G. Doğu, I. Ar, T. Doğu, 2003. "Breakthrough Analysis of H_2S Removal On Cu-V-Mo, Cu-V, and Cu-Mo Mixed Oxides", Chem. Eng. Comm. Vol. 190, pp. 1055-1072.

[41] S.C. Jain, R. Gupta, S.K. Gangwal, 1991. "Development of Zinc Ferrite Sorbents for Desulfurization of Hot Coal Gas in a Fluid-Bed Reactor", Paper Presented at AICheE Summer National Meeting, Pittsburgh, Pennsylvania.

[42] W. Mojtahedi, J. Abbasian, 1995. "H_2S Removal from Coal Gas at Elevated Temperature and Pressure in Fluidized Bed with Zinc Titanate Sorbents. 1. Cyclic Tests", Energy & Fuels. Vol. 9, pp. 429-434.

[43] R.E. Ayala, S.C. Jain, 1992. "Development of Durable Mixed-Metal Oxide Sorbents for High-Temperature Desulfurization of Coal Gases in Moving-Bed Reactors", Paper Presented at the AIChE 1992 Annual Meeting.

[44] R.B. Slimane, J. Abbasian, 2000. "Copper-Based Sorbents for Coal Gas Desulfurization at Moderate Temperatures", Ind. Eng. Chem. Res. Vol.39, pp. 1338-1344.

[45] A.B.M. Heesink, 1994. "High Temperature Coal Gas Desulphurization", Ph.D. Thesis, University of Twente, the Netherlands.

APPENDIX A

CALIBRATION CURVES AND METHOD USED IN GC

GC	: VARIAN CP-3800 Gas Chromatograph
Detector	: PFPD
Column type	: CP-Sil 5 CB for sulfur
Injector type	: 1177 with gas valve
Sample size	: 1 ml
Split ratio	: 50
Injector temperature	: 110^{o}C
Detector temperature	: 200^{o}C
Column temperature	: 80^{o}C
Carrier gas	: Helium
Inlet pressure	: 10 psi
Carrier gas flow rate	: 2 ml/min
Detector range	: 10
Fuel gas	: Hydrogen
H_2 flow rate	: 13 ml/min
Air flow rate (1)	: 17 ml/min

Air flow rate (2)	: 10 ml/min
Selectivity	: $\geq 10^6$ S/Carbon
Detectivity	: 1 pg S/sec

Calibration Curve
File:
Detector: 3800 GC, Address: 44, Channel ID:

H_2S

External Standard
Curve Type:
Origin:
y =

Resp. Fact. RSD:
Coeff. Det.(r^2):

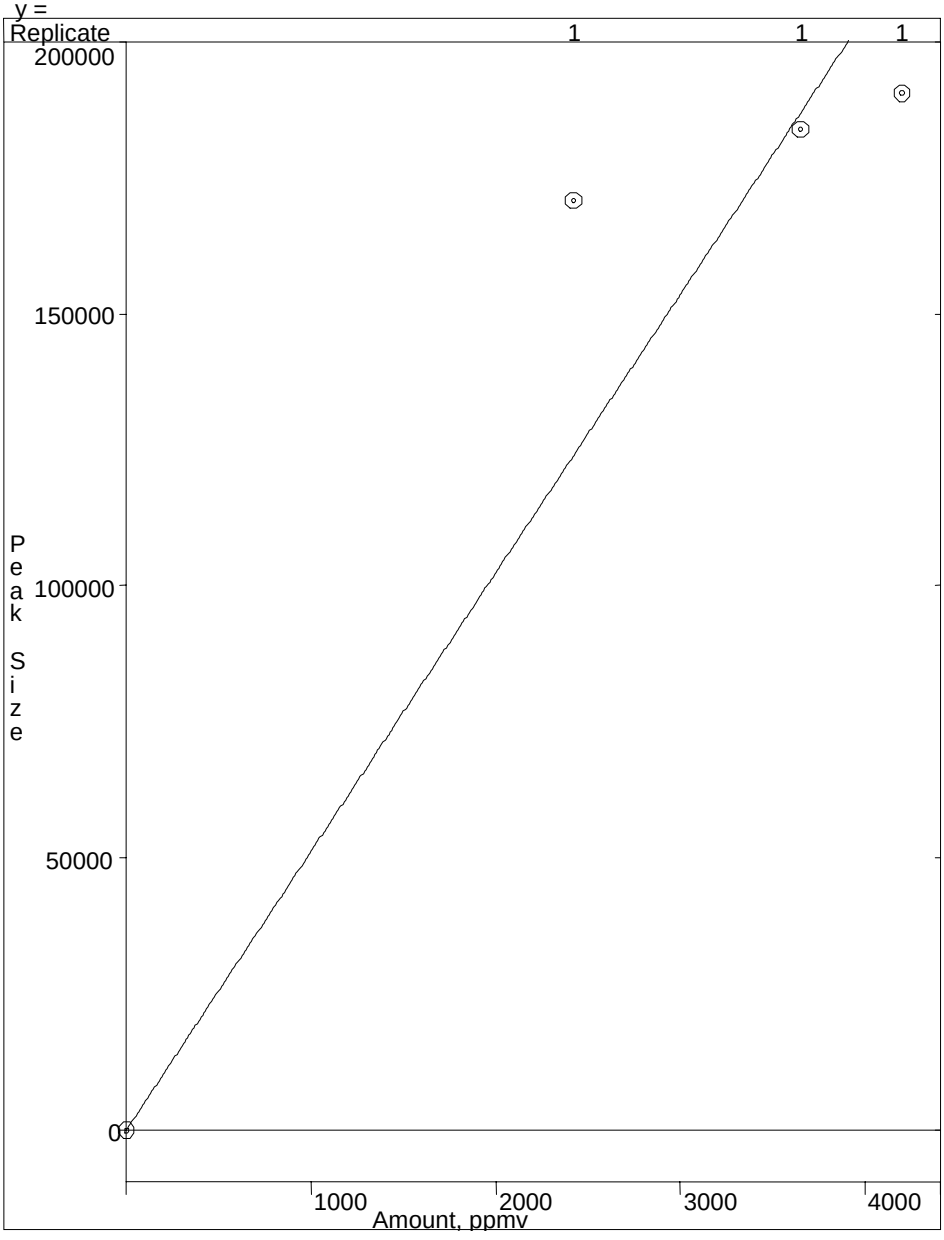

Figure A.1 Calibration Curve for H_2S

Calibration Curve Report
File: c:\star\so2.mth
Detector: 3800 GC, Address: 44, Channel ID:

SO_2

External Standard
Curve Type: Linear
Origin: Force
y = +1.794972e+003x

Resp. Fact. RSD:
Coeff. Det.(r^2): 0.915723

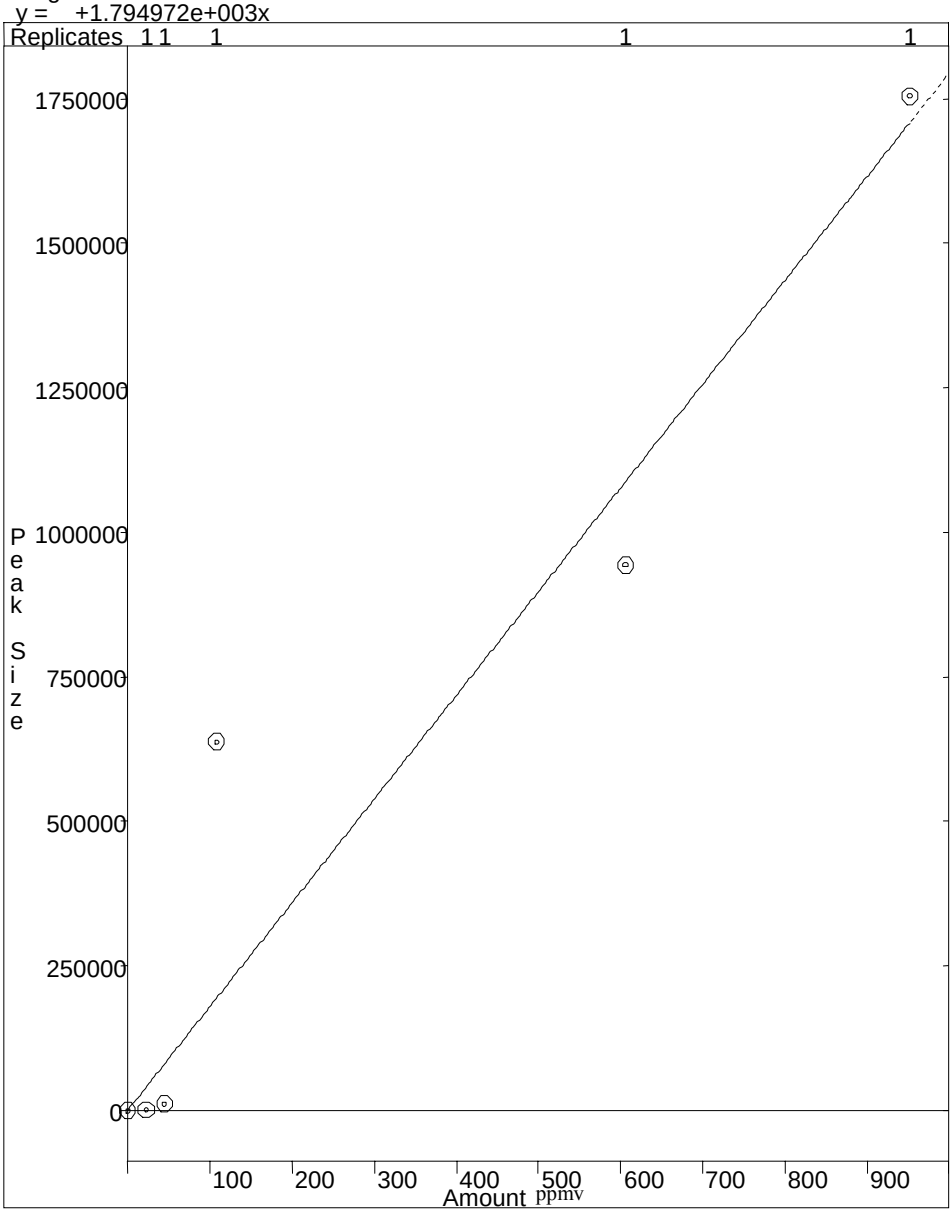

Figure A.2 Calibration Curve for SO_2

APPENDIX B

CALCULATION OF SORPTION CAPACITY

Breakthrough curves are obtained by plotting the exit H_2S concentration against the reaction time in the sulfidation experiments. Sorption capacities of the slags are calculated using these breakthrough curves. A typical breakthrough curve is given in Figure B.1. The area hatched in the figure shows the amount of H_2S sorbed during sulfidation.

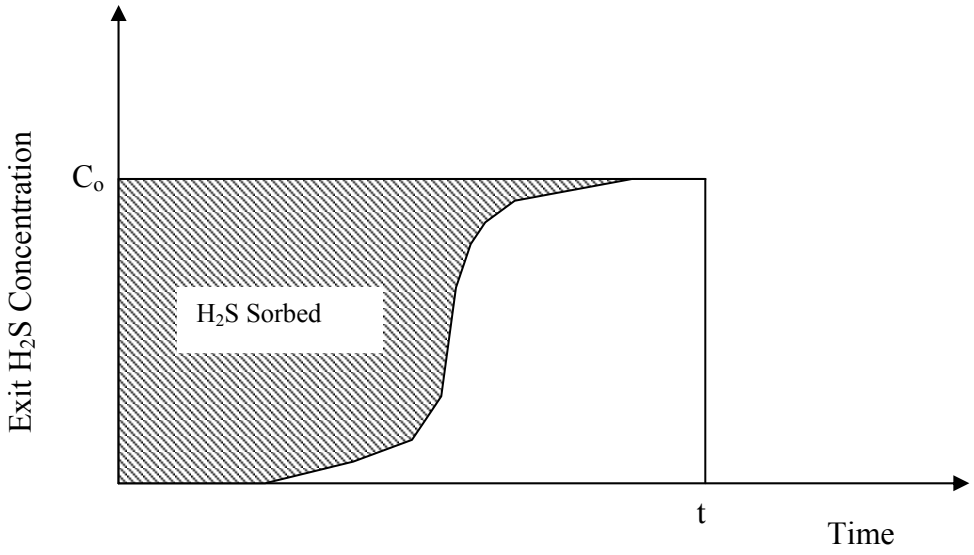

Figure B.1 Typical Breakthrough Curve

The area below the breakthrough curves is calculated by using trapezoidal method by means of an Excel sheet on the computer and the calculated area is subtracted from the total rectangular area to obtain the area above the curve.

As an example, the sorption capacity of steel slag at the temperature of 500°C with 3000 ppmv inlet H_2S concentration is calculated below.

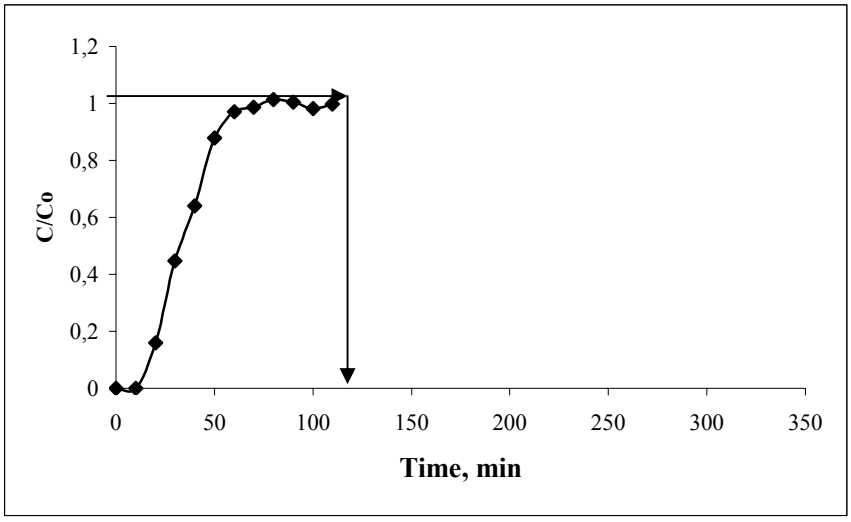

Figure B.2 Breakthrough Curve at 500°C with 3000 ppmv H_2S (Steel Slag)

Total sulfidation time = 110 min

At t = 110 min, $C/C_o = 1$

Total area = (110 min) x 1 = 110 min

Area under the curve = 75.79 min

Area above the curve = 110 – 75.79 = 34.21 min

Total gas flow rate (25°C, 1 atm) = 204.17 ml/min

Inlet concentration of H_2S = 3000 ppmv (0.3% by volume)

Flow rate of H_2S during the experiment=(204.17 ml/min)x0.003=0.612 ml/min

Total volume of H_2S = (0.612 ml/min) x 110 min = 67.37 ml

Density of H_2S @25^oC, 1 atm = 0.0014043 g/ml

Total mass of H_2S = 67.37 ml x 0.0014043 g/ml = 0.0946 g

Amount of H_2S sorbed = (0.0946 g) x 34.21 / 110 = 0.0294 g

Molecular weight of H_2S = 34 g

Amount of sulfur sorbed = 0.0294 g x (32/34) = 0.02769 g

Amount of sorbent used in sulfidation = 15 g

Sorption capacity = 0.02769 g x (100 g / 15 g) = 0.18 g S / 100 g Sorbent